EXHIBIT E

COPY OF "DERMAL PATHOLOGY," ED. J H GRAHAM, W C JOHNSON, AND E B HELWIG, HARPER-ROW, HAGERSTOWN, MD, CHAPTER 6 "BASIC PATHOLOGIC CHANGES IN SKIN" BY JAMES H GRAHAM, SEE PP 119-135, 125-126 (1972)

Edited by

James H. Graham, M.D.

Professor of Medicine (Dermatology), Department of Medicine, Chairman, Division of Dermatology, Professor of Pathology, Department of Pathology, Director, Section of Dermal Pathology, University of California, Irvine; Head, Section of Dermatology, Orange County Medical Center, Orange, California.

Waine C. Johnson, M.D.

Professor of Dermatology, Associate Professor of Pathology, Temple University School of Medicine; Director of Dermal Pathology Laboratory, Skin and Cancer Hospital of Philadelphia, Philadelphia, Pennsylvania.

Elson B. Helwig, M.D.

Chief, Department of Pathology and Branch of Dermal and Gastrointestinal Pathology, Washington, D.C.; Visiting Professor of Pathology in Dermatology, Temple University Health Sciences Center, Philadelphia, Pennsylvania; Clinical Professor of Pathology (Dermal), George Washington University School of Medicine, Washington, D.C.

With 17 Contributors

With 1155 Illustrations, 9 in Color

Dermal Pathology

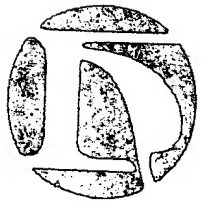

Medical Department

Harper & Row, Publishers
Hagerstown, Maryland
New York, Evanston, San Francisco, and London

First Edition

Standard Book Number: 06–141015–2

Library of Congress Catalog Card Number: 72-83366

6

Basic pathologic changes in skin

JAMES H. GRAHAM

The descriptive language of pathologic skin changes is unique in many respects when compared to terminology used in general pathology and deserves separate consideration to guide physicians preparing for specialty boards, and particularly pathologists and dermatologists interested in dermal pathology. The purpose of this chapter is to list important microscopic basic pathologic changes which characterize skin diseases by altering the epidermis, dermoepidermal junction, adnexal structures, dermis, and subcutaneous tissue. A workable definition is given for each term and several cutaneous diseases are listed which show the particular tissue alteration. Wherever possible at the end of each definition, the various basic pathologic changes will be keyed to specific photomicrographs used in different chapters which illustrate individual skin diseases. The complete list of selected photomicrographs appears right before the references at the end of the chapter. Publications which the readers may utilize for information on basic pathologic skin tissue changes are also listed.[1–5]

Epidermis

Hyperkeratosis

This change represents an increase in thickness of the stratum corneum. If caused by excessive formation of keratin there is usually hypergranulosis as seen in lichen planus, lichen simplex chronicus and lupus erythematosus. If caused by abnormal retention of the stratum corneum, the granular layer is usually normal or may be diminished to absent as occurs in ichthyosis vulgaris and ichthyosis congenita. Hyperkeratosis may be absolute as characterized by lichen planus or associated with parakeratosis which occurs in psoriasis and lichen simplex chronicus. Relative hyperkeratosis indicates an apparent

but not a true increase in thickness of the stratum corneum because of the degree of epidermal atrophy (Figs. 7–16A, 7–21*).

Follicular Plugging or Poral Hyperkeratosis

There is an increased amount of horny material or keratin in dilated pilosebaceous follicle ostia and/or sweat pores. Classic examples of diseases showing this change are lupus erythematosus, lichen sclerosus et atrophicus, keratosis pilaris, lichen spinulosus of Crocker, trichostasis spinulosa, lichen planopilaris, pityriasis rubra pilaris, and porokeratosis of Mibelli (Figs. 7–3, 7–21).

Delling

The surface of the epidermis shows a small depression, space, or hollow usually associated with hyperkeratosis, and this change occurs independent of sweat pores and pilosebaceous follicle ostia. Delling is seen particularly in lupus erythematosus and lichen sclerosus et atrophicus (Figs. 35–4, 35–5A).

Hypokeratosis

The term indicates a diminished thickness or thinning of the stratum corneum. This change can be seen in aging skin, erythroplasia of Queyrat, and dermatitis eczema diseases such as the acute and subacute stages of contact dermatitis, nummular eczema, seborrheic dermatitis, pityriasis rosea, parapsoriasis en plaques, lichen simplex chronicus with eczematous changes, papular lesions of atopic dermatitis and exfoliative dermatitis. In general, hypokeratosis is seen in eczematous weeping eruptions and cutaneous diseases which involve anatomic locations where there is a moist environment and opportunity for maceration (Figs. 7–3, 7–4A).

Parakeratosis

This change occurs in many skin diseases and reflects imperfect or abnormal keratinization of epidermal or adnexal keratinocytes. Parakeratosis is characterized by retention of nuclei in the stratum corneum or within the hair canal. In areas beneath prominent parakeratosis, the granular layer is usually thinned or absent. This latter change is well illustrated in psoriasis and Bowen's disease. Spotty or spotted parakeratosis characterizes verruca vulgaris and a number of inflammatory dermatoses such as lichen simplex chronicus, atopic dermatitis, and seborrheic dermatitis. Spotted parakeratosis at fairly regular intervals is seen particularly in pityriasis rosea, parapsoriasis guttata, parapsoriasis en plaques, and parakeratosis variegata. In some lesions of verruca vulgaris, verruca plantaris, and verruca palmaris, affected cells containing intranuclear inclusion bodies may be present in the thickened stratum corneum associated with parakeratosis. In some cutaneous diseases, melanin pigment may be associated with retained nuclei and the term "pigmented parakeratosis" has been used to characterize this combination. The terminology of pigmented parakeratosis is sometimes used when large amounts of melanin occur in the horny layer overlying certain nevus cell nevi and malignant melanoma, but retained keratinocyte nuclei are lacking. Diseases with prominent hypergranulosis, such as lichen planus, can sometimes show retention of keratohyaline granules in the stratum corneum and give a false type of parakeratosis (Figs. 7–16A, 7–21).

Hypergranulosis

This change is characterized by an increase in thickness of the granular layer and is usually seen in diseases showing hyperkeratosis from an abnormal production of horny material such as in lichen planus, lupus erythematosus, poikiloderma atrophicans vasculare, verruca vulgaris, verruca plana, lichenified lesions of atopic dermatitis, lichen simplex chronicus, and congenital ichthyosiform erythroderma. The term of relative hypergranulosis is sometimes used to describe diseases such as lichen sclerosus et atrophicus, since there is an apparent but not a true increase in thickness of the granular layer because of an extreme degree of epidermal atrophy (Figs. 7–16A, 7–52A).

* Complete figure citations are listed under each definition before the references at the end of the chapter.

Hypogranulosis

Thinning or absence of the granular layer characterizes hypogranulosis. This change is seen particularly in diseases showing prominent parakeratosis, such as psoriasis and Bowen's disease. Ichthyosis vulgaris and ichthyosis congenita may show hypogranulosis even though parakeratosis is lacking (Figs. 7–62, 7–65).

Superficial Crusting

This term is used to signify collections of inflammatory cells, red blood cells, fibrin, and plasma in the horny layer and stratum granulosum. Granular cells are usually diminished to absent and sometimes the stratum corneum is thinned or replaced by the exudate. Depending on the cutaneous disease, areas of superficial crusting may show colonies of bacteria, degenerating keratinocytes, fragments of hair, parakeratosis, and even tumor cells. Superficial crusting represents a common change in dermatitis eczema diseases and impetigo contagiosa. Some lesions of mycosis fungoides show tumor cells extending from Pautrier microabscesses to contribute to the contents of focal areas of superficial crusting (Figs. 7–21, 7–34A).

Acanthosis

Acanthosis indicates an increase in thickness of the stratum malpighii. The stratum malpighii includes the stratum basale (stratum germinativum) and stratum spinosum (prickle cell layer or spinous layer); therefore, acanthosis represents a thickening or increase in keratinocytes from the stratum granulosum to the epidermal basal layer. The term acanthosis also applies to the pilary complex when there is hyperplasia of adnexal keratinocytes of the pilosebaceous acrotrichium and follicular infundibulum. A uniform or regular acanthosis is best illustrated in psoriasis. An irregular type of acanthosis is usually seen in lichen simplex chronicus and chronic stages of other diseases in the dermatitis eczema group (Figs. 1–32, 5–6E).

Epidermal Collarette

This change shows elongated acanthotic rete ridges at the lateral margins of a pathologic alteration in the epidermis or dermis. The affected rete ridges usually curve toward the center of the lesion which may appear pedunculated. Collarette formation is seen in granuloma pyogenicum, senile angioma, angiokeratoma, fibroepithelial polyp, lichen nitidus, verruca vulgaris, keratoacanthoma, colloid milium, myxoid cyst, calcinosis cutis circumscripta, lymphangioma circumscripta, and nodular lesions of Kaposi's sarcoma (Figs. 17–7, 23–1).

Pseudoepitheliomatous Hyperplasia

The term means an extreme or prominent degree of irregular acanthosis mimicking carcinoma. The epidermal proliferation may show hyperplasia of either squamous cells or basal cells, but the keratinocytes appear uniform and there is a tendency for normal maturation. The pilary outer root sheath keratinocytes are often involved in cutaneous diseases showing pseudoepitheliomatous hyperplasia. A hyperplasia of squamous cells is commonly associated with exudative and infectious granulomas, ulcer margins, burns, and, sometimes, overlying lesions of granular cell myoblastoma. Basal keratinocyte hyperplasia mimicking multicentric basal cell carcinoma may be seen overlying some dermatofibromas and other skin lesions showing reactive fibrous connective tissue hyperplasia (Figs. 7–87, 7–88A).

Epidermal Atrophy

This change shows a decrease in thickness of the stratum malpighii. Epidermal atrophy is seen in poikiloderma of various types, atrophic lichen planus, lupus erythematosus, lichen sclerosus et atrophicus, and acrodermatitis chronica atrophicans (Figs. 7–108A, 8–1).

Thinning of Suprapapillary Epidermal Plates

This feature indicates epidermal atrophy overlying individual dermal papillae. This change is

frequently seen in psoriasis, Reiter's disease, keratoderma blennorrhagica and some other diseases which show papillomatosis (Fig. 11–26A).

Vacuolation

This change is characterized by formation of a space or cavity within altered cells. The affected cells appear clear or "washed out." There is usually evidence of cell injury such as epidermal keratinocyte alterations caused by certain cutaneous viral diseases, contact dermatitis, acute epidermal necrolysis, burns, and lupus erythematosus. Vacuolated cells are a normal feature of mucous membrane epithelium (Figs. 7–89B, 7–108A).

Epidermolysis or Epidermolytic Changes

These terms are synonymous and used in dermal pathology as descriptive ones to indicate cytologic changes of peculiar ballooning vacuolar granular degeneration of malpighian cells at various epidermal levels. Most epidermolytic diseases exhibit an increase in keratohyaline granules and some show bullae with epidermal separation in large sheets. Cutaneous diseases which show epidermolytic changes in some stage or phase include epidermolysis bullosa simplex, congenital ichthyosiform erythroderma of the bullous type, pachyonychia congenita, familial keratoderma palmaris et plantaris, verruca vulgaris, verruca plantaris, verruca palmaris, verruca plana, erythrasma, and some localized and systematized forms of epithelial nevi. As a coincidental occurrence, epidermolytic changes are sometimes observed in histologic sections of other cutaneous diseases. The affected cells in these cases show an increase in keratohyalin and the epidermolytic changes are often localized in relationship to the acrosyringium (Figs. 9–1, 9–3).

Necrolysis or Necrolytic Changes

This term indicates epidermal cell death of an acute type from a variety of etiologic agents. The altered stratum malpighii stains acidophilically, whereas the horny layer is colored basophilically, and this represents a reversal of the usual reaction of these structures. Pyknosis, vacuolar changes, acantholysis, and cellular degeneration account for intraepidermal separation at various levels in most cutaneous necrolytic diseases. Necrolytic changes are the principal basis for pathologic alteration in acute epidermal necrolysis, dermatitis exfoliativa neonatorum, second degree thermal injuries, acute radiodermatitis, and acute barbiturate intoxication reactions of the skin (Figs. 8–1 to 8–13).

Liquefaction Degeneration or Hydropic Degeneration of Basal Cells

This change represents a type of degeneration which causes vacuolization and disintegration of basal cells. The dermoepidermal basement membrane is indistinct or destroyed, and squamous cells are adjacent to the papillary corium. This alteration occurs in lupus erythematosus, lichen planus, lichen sclerosus et atrophicus, balanitis xerotica obliterans, various types of poikiloderma, incontinentia pigmenti, lichenoid drug eruption, polymorphous light eruption, erythema multiforme, pityriasis rubra pilaris, pityriasis lichenoides et varioliformis acuta, lichen striatus, and lichen nitidus. Liquefaction degeneration may cause subepidermal bulla formation in diseases such as lupus erythematosus, lichen planus, lichenoid drug eruption, and erythema multiforme. "Max Joseph spaces" represent microscopic clefts which occur at the dermoepidermal junction as a result of severe liquefaction degeneration, and these are particularly seen in lichen planus and some examples of lichenoid drug eruption (Figs. 7–39, 8–1).

Saw-Toothing

The alteration referred to as saw-toothed appearance is characterized by a triangular or angulated configuration of elongated pointed rete ridges. This feature is particularly seen in lichen planus and lichenoid drug eruption, and to a lesser extent in other diseases showing liquefaction degeneration (Figs. 9–36, 9–41).

Intercellular Edema or Spongiosis

This common change is characterized by edema between keratinocytes. The edema fluid causes an increase in width separating individual epidermal keratinocytes or adnexal keratinocytes from adjacent similar cells. The intercellular bridges or desmosomes are usually well defined and appear stretched. This change frequently occurs in inflammatory dermatoses, and is particularly a feature of dermatitis eczema diseases. Spongiosis is an important basic pathologic change in the pathogenesis of intraepidermal vesicle formation in diseases such as contact dermatitis, nummular eczema, pompholyx, allergic vesicular id eruption, vesicular dermatophytosis, acrodermatitis enteropathica, pityriasis rosea and polymorphous light eruption of the eczematous or contact type (Figs. 1–8, 7–34A).

Intracellular Edema or Alteration Cavitaire

This term refers to edema within cells of the stratum malpighii and/or adnexal keratinocytes. If severe, intracellular edema results in reticular degeneration of the affected cells. This change is seen in contact dermatitis, nummular eczema, pompholyx, allergic vesicular id eruption, vesicular viral diseases, vesicular stage of incontinentia pigmenti, and vesicular lesions of lichen striatus, pityriasis rosea, and dermatophytosis. Intracellular edema and spongiosis occur as common features in dermatoses showing intraepidermal vesicle formation (Figs. 7–35A, 7–35B).

Reticular Degeneration

This term indicates severe intracellular edema eventuating in the rupture of epidermal cells and/or adnexal keratinocytes. The resisting cell membranes collapse upon each other and form multiple septa. In general, this change results in multilocular intraepidermal vesicles and bullae. Reticular degeneration plays an important role in the formation of vesicles and bullae in cutaneous viral diseases, contact dermatitis, dermatophytosis, nummular eczema, allergic id eruption, pompholyx, lichen striatus, incontinentia pigmenti, and pityriasis rosea. The terminology of reticular degeneration should not be confused with dermal alterations affecting connective tissue reticulum fibers or reticular cells (Figs. 7–35A, 7–35B).

Ballooning Degeneration

Ballooning degeneration is a descriptive term which refers to swelling of epidermal cells and/or adnexal keratinocytes. The change is caused by prominent intracellular edema and results in acantholysis with formation of intraepidermal vesicles and bullae. The term is used primarily in reference to cutaneous viral diseases such as herpes simplex, varicella, herpes zoster, variola, vaccinia, ecthyma contagiosum (orf) and milkers nodule. Ballooning degeneration represents a prominent change in varicella, herpes zoster and herpes simplex, and usually results in unilocular intraepidermal vesicles. Lesions of variola and vaccinia are characterized more by reticular degeneration with formation of intraepidermal multilocular bullae (Figs. 9–1, 9–7).

Acantholysis

Acantholysis indicates loss of cohesion between epidermal cells and/or adnexal keratinocytes due to degeneration or faulty formation of intercellular bridges (desmosomes). This change or defect leads to formation of intraepidermal slits, clefts, lacunae, vesicles and bullae. Acantholysis occurs in pemphigus vulgaris, pemphigus vegetans, pemphigus erythematosus, pemphigus foliaceus, fogo selvagem, familial benign chronic pemphigus, herpes simplex, varicella, herpes zoster, variola, vaccinia, keratosis follicularis (Darier's disease), isolated dyskeratosis follicularis (warty dyskeratoma), solar keratosis, and adenoid squamous cell carcinoma (adenoacanthoma). Acantholysis may be seen as a nonspecific feature in many pustular, vesicular, and bullous diseases, and particularly those showing large numbers of polymorphonuclear leukocytes and/or bacteria. Many acantholytic cells can be demonstrated in some examples of impetigo contagiosa, subcorneal pustular dermatosis and acute epidermal necrolysis. Acantholytic cells are more easily demonstrated in intraepidermal pustular,

vesicular, and bullous diseases, but may also be seen in diseases showing subepidermal bullae such as dermatitis herpetiformis, bullous pemphigoid, and erythema multiforme with prominent liquefaction degeneration. Occasionally, anaplastic forms of intraepidermal epithelioma of Jadassohn show focal areas of acantholysis (Figs. 8–4, 8–5).

Vesicle or Bulla

A small bulla is generally called a vesicle, and the terms refer to primary skin lesions characterized by cavities forming in a subcorneal location, intraepidermally at various levels, at the dermoepidermal junction, or subepidermally. Bullae are filled with plasma, often inflammatory cells, and may contain keratinocytes and other contents. Subcorneal bullae are seen in impetigo contagiosa and subcorneal pustular dermatosis. Superficial intraepidermal acantholytic bullae occur in pemphigus erythematosus, whereas pemphigus vulgaris and familial benign chronic pemphigus show suprabasilar separation. Intraepidermal bullae showing multilocular features are seen in contact dermatitis and variola, whereas the unilocular type is more common in herpes simplex and herpes zoster. Bullae developing in the region of the dermoepidermal interface are best illustrated by dermatitis herpetiformis, bullous pemphigoid, and epidermolysis bullosa hereditaria letalis. Bullous dermatoses showing separation in the papillary corium are characterized by the recessive type of epidermolysis bullosa dystrophica, porphyria cutanea tarda, and erythema multiforme. Microscopic slit-like bullae occur in Darier's disease and solar keratosis with acantholysis, and these intraepidermal spaces are referred to as lacunae or clefts (Figs. 7–37A, 7–61).

Dyskeratosis

This term indicates imperfect or abnormal keratinization of individual epidermal cells and/or adnexal keratinocytes. There are two types of dyskeratosis, one occurring in benign abnormal keratinizing diseases and the other in premalignant and malignant cutaneous epithelial lesions showing an atypical hyperplasia of keratinocytes. Keratinization of individual cells may occur at all epidermal levels. Keratinocytes of the acrotrichium, follicular infundibulum, and acrosyringium may be affected in a similar way. Benign dyskeratosis commonly occurs in isolated dyskeratosis follicularis and Darier's disease in the form of corps ronds and grains. Benign dyskeratosis occurs in familial benign chronic pemphigus and pemphigus erythematosus, but the change is best demonstrated by electron microscopy. Malignant dyskeratosis occurs in the form of premature and atypical keratinization of individual cells in Bowen's disease, erythroplasia of Queyrat, leukoplakia, leukoplakia with squamous cell carcinoma, solar keratosis, solar keratosis with acantholysis, solar keratosis with squamous cell carcinoma, x-ray keratosis, x-ray keratosis with squamous cell carcinoma, de novo squamous cell carcinoma, some types of adnexal carcinoma, and adenoid squamous cell carcinoma. Individual cell keratinization may also be seen in keratoacanthoma, intraepidermal epithelioma of Jadassohn, incontinentia pigmenti, pemphigus foliaceus, pemphigus vegetans, and, to a minor degree, in a variety of other cutaneous diseases. Malignant dyskeratosis may affect atypical keratinocytes involving the superficial dermis, deep corium, and metastatic sites in squamous cell carcinoma, adenoid squamous cell carcinoma, and some precancerous lesions which invade the stroma as carcinoma. In general, malignant dyskeratosis is not seen in basal cell carcinoma, but this change may occur in the metatypical or basosquamous type. Malignant dyskeratosis is not seen in mammary Paget's disease or extramammary Paget's disease (Figs. 9–2B, 9–5).

Anaplasia

In reference to cutaneous premalignant or malignant neoplasms, anaplasia indicates atypical cellular maturation or reversion to an undifferentiated state. Anaplastic cells have large, hyperchromatic, irregularly shaped nuclei, often prominent nucleoli, and frequently they show

atypical mitotic figures. There may be loss of cohesion of the cells for each other (Figs. 1–26, 20–18).

Dysplasia

This term broadly represents an abnormal state or faulty condition of development and is sometimes used in dermal pathology as a descriptive one to identify atypical cellular changes in precancerous skin lesions (Figs. 1–26, 24–1).

Nesting or Theques of Cells

This feature refers to aggregates, groups, or nests of cells located in the epidermis, acrotrichium, follicular infundibulum, acrosyringium and/or corium. The term applies predominantly to a proliferation of keratinocytes or neuroepithelial structures, and the cellular nests are usually sharply delineated from adjacent adnexal, malpighian and mesenchymal structures. The nests of cells may show a whorl-like pattern. Cellular nesting is a feature seen in intraepidermal epithelioma of Jadassohn, irritated seborrheic keratosis, inverted follicular keratosis, keratoacanthoma, squamous cell carcinoma, isolated dyskeratosis follicularis, epidermoid cyst with pseudoepitheliomatous hyperplasia, epithelial nevi, cellular nevi (nevus cell nevi), malignant melanoma, eccrine poroma, eccrine porosyringoma (acrospiroma), mammary Paget's disease, extramammary Paget's disease, some types of metastatic carcinoma, solar keratosis, and Bowen's disease. Theque is a common term used for epidermal and dermoepidermal nests of nevus cells occurring in junction and compound cellular nevi. The horn pearls of squamous cell carcinoma and squamous eddies seen in inverted follicular keratosis are examples of aggregates or whorls of epidermal and adnexal keratinocytes, respectively (Figs. 5–15, 20–3).

Squamous Eddy

Squamous eddy formation implies a whorl-like pattern of squamoid cells in areas of keratinocyte hyperplasia in inverted follicular keratosis and inflamed lesions of seborrheic keratosis. The epithelial cells forming squamous eddies do not show atypism or evidence of dyskeratosis. Squamous eddy formation may be seen in keratoacanthoma, intraepidermal epithelioma of Jadassohn, lichenoid benign keratosis, isolated dyskeratosis follicularis, inflamed epithelial nevi, eccrine poroma and eccrine porosyringoma. In some benign cutaneous keratoses, squamous eddy formation may represent a reactive response to irritation or other stimuli. The change probably results from basal cells and/or adnexal cells showing squamous maturation (Figs. 11–7, 23–11B).

Horn Cysts

These structures are also called keratin cysts or keratin tunnels and represent concentrically arranged keratinized centers surrounded by flattened epidermal keratinocytes or adnexal cells. The epithelial cell hyperplasia associated with horn cysts is usually basaloid in type but may appear squamoid. Horn cysts are seen in seborrheic keratosis, solitary trichoepithelioma, epithelioma adenoides cysticum of Brooke, basal cell carcinoma, nevoid basal cell carcinoma, intraepidermal epithelioma of Jadassohn, epithelial nevi and some cellular nevi (Figs. 23–9, 23–10).

Squamous Pearls

These structures are also referred to as horn pearls and represent concentric layers of atypical squamous keratinocytes showing gradual keratinization toward the central part. Horn pearls exhibit anaplastic and malignant dyskeratotic cells, and are particularly seen in differentiated types of squamous cell carcinoma (Figs. 24–14, 24–17).

Exocytosis

This term simply indicates migration of inflammatory cells from the dermis into the epidermis and/or adnexal structures. Exocytosis is particularly seen in diseases of the dermatitis eczema group (Figs. 7–36A, 7–39).

Microabscess

Microabscesses represent small accumulations of polymorphonuclear leukocytes or lymphoid cells in the epidermis and/or adnexal structures. A Munro microabscess contains neutrophils and is usually seen at the granular cell level, but may be located in the stratum malpighii or horny layer. Munro microabscesses are commonly seen in psoriasis but also occur in pustular bacterid, acrodermatitis continua of Hallopeau, pustulosis palmaris et plantaris, primary irritant contact dermatitis, Reiter's disease, keratoderma blennorrhagicum, impetigo contagiosa, subcorneal pustular dermatosis, miliaria pustulosa, some examples of seborrheic dermatitis, early stages of parapsoriasis guttata, cutaneous candidiasis, and dermatophytosis. The Pautrier microabscess is seen in mycosis fungoides and contains malignant monocytoid reticuloendothelial cells. Pautrier microabscesses are usually located in the main part of the stratum malpighii, but may involve superficial epidermal levels, dermoepidermal junction, and pilary outer root sheath. Pautrier microabscesses are located at the dermoepidermal junction particularly when there is liquefaction degeneration as occurs in mycosis fungoides with poikiloderma. Pautrier-type microabscesses representing small epidermal collections of mononuclear lymphoid cells may be seen in lichen simplex chronicus, atopic dermatitis, nummular eczema, pityriasis rosea, allergic contact dermatitis, allergic id eruption, parapsoriasis en plaques, parakeratosis variegata, older lesions of parapsoriasis guttata, and erythema perstans. Microabscesses containing eosinophilic leukocytes occur in the epidermis or adnexal structures in erythema toxicum, incontinentia pigmenti, pemphigus vegetans, dermatitis vegetans, scabies, and creeping eruption. In dermatitis herpetiformis, small collections of eosinophils and/or neutrophils occur at the dome of some dermal papillae, and these cells may also be present in the adjacent epidermis (Figs. 7–40, 7–41A).

Abscess

Macroabscesses are seen grossly as pustules and contain many neutrophils. Macroabscesses are located intraepidermally in diseases such as pustular psoriasis, pustular bacterid, pustulosis palmaris et plantaris, acrodermatitis continua of Hallopeau, Reiter's disease and keratoderma blennorrhagicum. The multiloculated spongioform pustule of Kogoj may occur in these diseases and probably represents an enlarged Munro microabscess. Miliary abscesses occur in areas of pseudoepitheliomatous hyperplasia and/or dermal granulomatous inflammation, and are seen grossly in exudative granulomas such as bromoderma, iododerma, granuloma inguinale, tuberculosis verrucosa cutis, and the deep mycoses (Figs. 7–4A, 7–22B).

Pyknosis

This change is characterized by shrinking and distortion of cell nuclei. As a result of pyknosis, the cytoplasm of affected cells usually appears "washed-out." Pyknosis particularly occurs when there is evidence of cell injury and is usually seen in diseases showing epidermal vacuolation changes such as acute second degree burn (Figs. 8–2, 8–3).

Karyorrhexis

This term indicates fragmentation of cell nuclei. Leukocytoclasis specifically means nuclear fragmentation of neutrophils. Chromatin dusting refers to fragmentation of nuclei of polymorphonuclear leukocytes and mononuclear cells into minute basophilic staining particles or granules. Karyorrhexis is seen in pustular dermatoses, pyoderma gangrenosum, exudative granulomas and diseases showing tissue reaction changes of allergic angiitis (Fig. 11–19B).

Hypopigmentation

Hypopigmentation indicates there is a decrease or absence of melanin pigment in the epidermal basal layer. This feature is seen in vitiligo, albinism, areas of postinflammatory depigmentation, occupational leukoderma, halo nevus and contact dermatitis from hydroquinone (Figs. 7–96A, 11–23).

Hyperpigmentation

This term is used synonymously with melanosis and indicates an increase in melanin pigment in the basal layer of the epidermis and/or upper corium. Melanosis is seen in Addison's disease, café au lait spots, chloasma, fixed drug eruption, areas of postinflammatory pigmentation, and may be seen associated with other pigmentary problems such as hemochromatosis and argyria (Figs. 11–16, 11–29A).

Incontinence of Pigment

This change indicates loss of melanin from the epidermal basal keratinocytes and altered melanocytes because of damage to these cells. Melanin accumulates in the upper corium where pigment granules are free and within melanophages. Dropping off of melanin occurs in incontinentia pigmenti, lichen planus, lupus erythematosus, poikiloderma atrophicans vasculare, Riehl's melanosis, melanodermatitis toxica, poikiloderma congenitale, lichen sclerosus et atrophicus, fixed drug eruption, lichenoid drug eruption, melanotic freckle of Hutchinson and diseases showing postinflammatory hyperpigmentation. Loss of epidermal melanin occurs particularly in diseases showing liquefaction degeneration, but incontinence of pigment may also be seen in other dermatoses (Fig. 11–31).

Dermis

Melanophage

This mesodermal cell is a specialized histiocyte, macrophage, or Schwann cell which engulfs melanin and acts as a pigment carrier. This cell is located in the corium and cannot produce melanin. Melanophages occur in cutaneous diseases which show incontinence of pigment (Figs. 20–1, 20–2).

Villi

This term refers to elongated and sometimes tortuous dermal papillae which are generally covered with one or two layers of malpighian keratinocytes or adnexal cells. These structures extend from the corium into the base of an intraepidermal vesicle, bulla, cleft, lacuna, or dermal cystic cavity. Villus formation is seen in isolated dyskeratosis follicularis, Darier's disease, familial benign chronic pemphigus, pemphigus vulgaris, pemphigus vegetans, syringadenoma papilliferum, hidradenoma papilliferum, and solar keratosis with acantholysis (Figs. 9–8, 9–9).

Festooning

Festooning indicates a continuous, joined together, undulating, looping, or curving configuration of dermal papillae projecting into the base of a bulla. This change is seen in bullous pemphigoid, benign mucosal pemphigoid, porphyria cutanea tarda, porphyria congenita, various types of epidermolysis bullosa dystrophica, epidermolysis bullosa hereditaria letalis, second degree burn, and some examples of acute epidermal necrolysis. This change can sometimes occur in dermatitis herpetiformis, localized chronic pemphigoid, and erythema multiforme (Figs. 8–6, 8–12).

Papillomatosis

This change is characterized by an upward proliferation of dermal papillae producing an irregular undulating pattern or configuration to the epidermis. This feature is seen in psoriasis, other inflammatory diseases, and a variety of cutaneous neoplasms (Figs. 7–52A, 7–88A).

Papilloma

This is a morphologic term used for tumor or tumor-like proliferations showing papillomatosis and hyperkeratosis. A combination of hyperkeratosis, papillomatosis and epidermal hyperplasia may be referred to as verrucous acanthosis. These changes are seen in verruca vulgaris, condyloma acuminatum, nevus verrucosus, some localized and systematized epithelial nevi, acrokeratosis verruciformis of Hopf, nevus sebaceus of Jadassohn, seborrheic keratosis, occasional lesions of solar keratosis, a few fibroepithelial

polyps, inverted follicular keratosis, and acanthosis nigricans (Figs. 23–4, 23–9).

Peripheral Palisading

This term indicates a palisaded arrangement of cell nuclei occurring at the margin of an alteration, necrobiotic change, infiltration, or cellular proliferation. This change occurs in the Verocay bodies of neurilemmoma and peripheral cell layer of islands and strands of basal cell carcinoma. In older lesions of granuloma annulare, necrobiosis lipoidica diabeticorum, rheumatic fever nodule, and beryllium granuloma, there is a tendency for palisading of fibrocytic and epithelioid cells at the periphery of necrobiotic areas (Figs. 16–1, 16–5).

Grenz Zone

In dermal pathology, this term indicates a marginal zone of relatively uninvolved connective tissue that separates the epidermis from an underlying alteration, cellular infiltrate, or tumor proliferation in the corium. This feature is seen in granuloma faciale, acrodermatitis chronica atrophicans, intradermal cellular nevus, some examples of urticaria pigmentosa, benign lymphocytic infiltration of Jessner, lymphocytoma cutis, reticulum cell sarcoma, leukemia cutis of various types, lymphocytic lymphoma cutis, solar elastosis, lepromatous leprosy, dermal eccrine cylindroma, pseudoxanthoma elasticum, colloid milium and cutaneous leiomyoma (Figs. 7–41A, 17–9).

Basophilic Degeneration of the Connective Tissue (Senile or Solar Elastosis)

This alteration shows an amorphous, granular, basophilic change of the papillary connective tissue. In some examples, the upper corium appears replaced or obscured by curling fibers in haphazard arrangement. A narrow grenz zone separates this change from the dermoepidermal junction. The material is tinctorially similar to elastic tissue and when special stains are utilized, the alteration is called senile elastosis or solar elastosis. Solar elastosis is not a specific change for any particular disease, and this alteration can be seen in tissue sections from areas of chronic actinic exposure. This alteration is not seen as a significant change in Negro skin unless there is preexisting hypopigmentation such as albinism, leukoderma, or vitiligo of sun exposed areas of the body (Figs. 24–1A, 24–3).

Homogenization

This term applies to dermal alterations characterized by an amorphous, smooth, uniform change of the connective tissue. The altered tissue change may stain basophilically or acidophilically, and appear pale, opaque, or translucent. Homogenization is seen in lichen sclerosus et atrophicus, balanitis xerotica obliterans, solar elastosis, chronic radiodermatitis, amyloidosis cutis, colloid milium, erythropoietic protoporphyria, lipoid proteinosis, chondrodermatitis nodularis chronica helicis, recessive type of epidermolysis bullosa dystrophica, and other diseases showing fibrinoid change (Figs. 8–15, 8–17).

Collagenolysis

This alteration indicates an homogenized appearance to a narrow subepidermal zone of papillary dermis as viewed by light microscopy. The terminology applies to collagenous degeneration such as occurs in epidermolysis bullosa dystrophica. Collagenolysis occurs in the dermis adjacent to the base of bullae which show prominent festooning and is particularly seen in epidermolysis bullosa dystrophica of the recessive type. By electron microscopy, collagenolysis shows fragmentation and granular degeneration of fibers, some of which are engulfed by macrophages (Figs. 9–1, 9–16).

Hyaline Degeneration

This term indicates an alteration or replacement of a preexisting structure to something which appears pellucid to glassy, and may be transparent or nearly so. Hyalin refers to a dermal translucent albuminoid substance occurring in amyloidosis cutis of various types. Hyaline ma-

terial is seen in dermal eccrine cylindroma, lipoid proteinosis, colloid milium, porphyria cutanea tarda, erythropoietic protoporphyria, lupus erythematosus, lichen planus and other diseases showing liquefaction degeneration (Figs. 22–6 to 22–9).

Fibrinoid Degeneration

This term, as applied to cutaneous diseases, indicates bands, clumps, and droplets of a complex, heterogenous, acidophilic, amorphous, acellular substance in tissue. Depending on the disease, the alteration may involve dermal connective tissue, extracellular interfibrillar ground substance, and blood vessels. Fibrinogen, other plasma proteins, immunoglobulins, and chemical changes in the connective tissue, ground substance and dermal blood vessels may be components of fibrinoid. Fibrinoid degeneration is seen in lupus erythematosus, chondrodermatitis nodularis chronica helicis and antihelicis, allergic angiitis, allergic granulomatosis, periarteritis nodosa, erythema elevatum diutinum, granuloma faciale, cutaneous sarcoidosis, rheumatic fever nodule, rheumatoid nodule, old lesions of granuloma annulare, thrombotic thrombocytopenic purpura, angiolipoma, and atrophie blanche of Milian. In general, fibrinoid of antigen-antibody precipitates stains like fibrin, but this is not a specific change since the Schwartzman phenomenon and other nonimmune diseases can give similar tissue alterations. The fibrinoid of lupus erythematosus, rheumatoid nodule, and rheumatic fever nodule contains immunoglobulins. In most types of lupus erythematosus, fluorescent rabbit antibodies specific for human fibrinogen give a negative reaction. An exception to this is lupus erythematosus profundus where fibrinoid sometimes occurs in the deep corium and subcutaneous tissue, and this substance shows histochemical characteristics of fibrin or fibrin precursor proteins. In sections of lupus erythematosus, hyaline material seen at the dermoepidermal junction, adnexal basement membrane sites and the walls of blood vessels show histochemical fluorescent characteristics of immunoglobulins. Small colloid droplets of fibrinoid are sometimes referred to as "Civatte bodies" and these hyaline clumps may be seen in the upper corium of diseases showing liquefaction degeneration. Civatte bodies may be seen in lupus erythematosus, polymorphous light eruption, lichen planus, lichenoid drug eruption, poikiloderma atrophicans vasculare, incontinentia pigmenti, and erythema multiforme (Figs. 7–45B, 11–14).

Necrobiosis

As applied to certain granulomatous dermatoses, necrobiosis indicates an alteration characterized by loss of normal staining ability of fibrocytes, fat cells, dermal connective tissue fibers, and blood vessels, but still showing some outlines of normal architecture and without appreciable inflammation. Dermal repair is usually evident adjacent to areas of necrosis in the form of a palisaded arrangement of fibrocytes and epithelioid cells. Necrobiosis is seen in granuloma annulare, necrobiosis lipoidica, necrobiosis lipoidica diabeticorum, rheumatoid nodule, rheumatic fever nodule, beryllium granuloma, and other foreign body granulomas that cause a granuloma annulare type of dermal connective tissue alteration (Figs. 7–43A, 16–1).

Caseation Necrosis

This is a type of tissue death in which the affected area has lost its structural characteristics, and the necrotic zone shows amorphous, fine granular material which stains a pale eosinophilic to basophilic color. Unless the necrosis is far advanced, some pyknotic nuclei are usually present within the involved sites. Areas of caseation necrosis show no appreciable invasion by inflammatory cells. This change is seen in some lesions of tertiary spyhilis, papulonecrotic tuberculid, acnitis, scrofuloderma and lupus miliaris disseminatus faciei (Figs. 13–12, 14–2).

Sclerosis

This dermal connective tissue change is characterized by a hypertrophic, compact, coarse, acel-

lular, acidophilic appearance of the collagen bundles. The usual fibrillar pattern of collagen is lacking. This alteration is seen in morphea, diffuse scleroderma, sclerodermatomyositis, chronic radiodermatitis, scleredema adultorum of Buschke and scleredema adultorum diutinum (Figs. 11–23, 11–30).

Dermal Atrophy

Dermal atrophy implies that the overall thickness of the corium is diminished from thinning of the collagen and/or elastic tissue, and there is usually absence of pilosebaceous follicles. Acrodermatitis chronica atrophicans represents an example of acquired dermal atrophy with thinning to absence of collagen, elastic fibers and pilosebaceous follicles. Dermal atrophy may result from hereditary or congenital absence of connective tissue such as seen in nevus lipomatosis superficialis. When dermal atrophy is prominent, large blood vessels, eccrine sweat glands and even fat tissue may be present in the superficial corium. Macular atrophy and stria are examples of dermal diseases showing degeneration or absence of elastic tissue (Fig. 31–18).

Elastorrhexis

This dermal alteration represents elastic tissue degeneration characterized by splintering, fragmentation, clumping and an amorphous, granular, basophilic appearance to the altered fibers. This change is illustrated in pseudoxanthoma elasticum, juvenile elastoma, and some examples of cutis laxa (Figs. 34–3, 34–7).

Interstitial Edema

This term indicates edema fluid separating the dermal connective tissue fibers. If present for any length of time, this change can cause splitting, thinning, and atrophy of collagen and elastic fibers. Interstitial edema is a feature seen in acute dermatoses, cellulitis, erysipelas, contact dermatitis, urticaria, burns, and most of the subepidermal bullous dermatoses (Figs. 7–9A, 7–12).

Mucinous or Myxoid Degeneration

This alteration is characterized by an amorphous, stringy, basophilic staining substance which separates, thins and replaces the dermal connective tissue fibers. Special histochemical techniques identify this substance as hyaluronic acid, although in some diseases, sulfated acid mucosaccharides or sialomucin are present and may represent the predominant material in areas of myxomatous alteration. This change is seen in myxedema, localized pretibial myxedema, papular mucinosis, focal mucinosis, myxoid cyst, ganglia, scleredema adultorum diutinum, Fox-Fordyce disease, lupus erythematosus, dermatomyositis, malignant atrophic papulosis (Degos' disease), plexiform neurofibroma, myxoma, adenocystic carcinoma (mucin secreting carcinoma of the skin), and a variety of other neoplasms (Figs. 7–32C, 7–32D).

Fatty Degeneration or Deposition

This alteration indicates infiltration of the skin by lipids. The fat deposits are primary or secondary in type, and the lipid material may be intracellular and/or extracellular. The lipids are located in the cytoplasm of xanthoma cells in xanthoma tuberosum, xanthelasma, and xanthoma diabeticorum. Fatty infiltration of the stroma by foamy appearing cells and extracellular lipid deposits represents a secondary change in lesions such as sclerosing hemangioma, fibroxanthoma, and necrobiosis lipoidica. Lipid deposition may be seen in a wide variety of cutaneous inflammatory, granulomatous, and reactive diseases (Figs. 32–2, 32–3).

Calcinosis

Calcinosis cutis is characterized by an amorphous, densely basophilic, granular material in the corium, and its occurrence is either metastatic or dystrophic (secondary) in type. Metastatic calcification is associated with primary or secondary disease of the parathyroid glands and there is usually hypercalcemia. Dystrophic calcinosis cutis may occur in pilar cyst, dermoid cyst,

epidermoid cyst, amyloid tumor, pilomatrixoma, scleroderma, dermatomyositis, pseudoxanthoma elasticum, cellular nevi, basal cell carcinoma, nevoid basal cell carcinoma, foreign body granuloma, solitary trichoepithelioma, and epithelioma adenoides cysticum of Brooke (Figs. 23–23, 23–29).

Pigmentation or Pigment Deposition

This change is characterized by dermal deposits of pigment other than melanin. Fine granules and/or irregular aggregates of pigment may be located in relationship to adnexal structures, blood vessels, nerves, and macrophages. The pigment may be endogenous or exogenous in origin. Hemosiderosis and hemochromatosis are examples of endogenous pigmentation, whereas coloring of the skin from exogenous granular material occurs in argyria and tattoos (Figs. 11–5 to 11–9).

Metachromasia

Metachromasia is the phenomenon of tissue, cells, or a substance reacting tinctorially different from that of the dye color used for staining. This is exhibited by mast cells in urticaria pigmentosa and the hyalin of amyloidosis cutis when dyes such as toluidine blue and crystal violet are used for staining (Fig. 35–7C).

Birefringence

When cutaneous tissue sections (paraffin or frozen), skin scrapings, or gross specimens such as hair are examined microscopically utilizing polarizer and analyzer polaroid lenses, certain particles, substances, and structures are characterized by being doubly refractive or anisotrophic. By gradually rotating the polarizer or analyzer lenses, the plane of polarized light is disrupted and the field appears dark. Particles, substances, and structures which exhibit birefringence appear brilliant white to yellow in a dark background when they are interposed between the two lenses. Collagen fibers, hard keratin of hair, and the stratum corneum normally show birefringence. Birefringence is also a pathologic feature of cutaneous diseases such as silica granuloma, talc granuloma, suture granuloma, gout granuloma, keratin granuloma, allergic red mercurial granuloma, foreign body granulomas containing vegetable matter, certain xanthomas rich in cholesterol esters (frozen sections are necessary), amyloidosis cutis, and colloid milium. Certain materials which exhibit birefringence also show dichroism, trichroism or polychroism. This phenomenon is characterized by a change in color of the anisotrophic compound by rotating the polarizer or analyzer lenses while keeping the specimen under direct observation. A yellow to green dichroism is seen in amyloidosis cutis, whereas trichroism occurs in colloid milium and this is characterized by color changes varying from yellow with shades of orange to blue-green. Plucked gross catagen hairs, and particularly club hairs from alopecia areata and telogen effluvium, show a wide spectrum of polychroism when examined polariscopically (Figs. 7–55A, 18–4).

Metaplasia

The term means an alteration or change of one type of tissue into another. A good cutaneous example of this occurrence is bone formation in epithelial tumors such as pilomatrixoma and nevoid basal cell carcinoma (Fig. 23–30).

Angiitis or Vasculitis

In dermal pathology these terms are synonymous and used for describing vascular changes of thickening, endothelial swelling, and infiltration of blood vessel walls by inflammatory cells. Eosinophils, neutrophils, and extravasated red blood cells are usually present, but not in all examples. There may be karyorrhexis and, if severe, chromatin dusting is seen. Angiitis is usually seen in dermal hypersensitivity reactions such as papular urticaria, drug reactions, persistent insect bite reaction, erythema multiforme, id reactions, anaphylactoid purpura, erythema elevatum diutinum, polymorphous light eruption, pityriasis lichenoides et varioliformis acuta,

and atrophie blanche of Milian (Figs. 7–36B, 7–37B).

Vascular Ectasia

This term indicates dilatation or an increase in diameter of vascular lumina. This change is seen in chronic radiodermatitis, lupus erythematosus, lichen sclerosus et atrophicus, poikiloderma of various types, hemangioma, lymphangioma, psoriasis, precancerous skin lesions, cutaneous carcinomas, verruca vulgaris, and a variety of other skin diseases (Figs. 7–41, 7–88A).

Vascular Obliteration

This term refers to intimal proliferation and/or thickening of blood vessel walls to the point of obliteration. Fibrinoid thrombi may sometimes be present. Vascular occlusion is seen in thromboangiitis obliterans, endarteritis of arteriosclerosis, scleroderma, chronic radiodermatitis, thrombophlebitis, periarteritis nodosa, allergic granulomatosis, lymphomatoid papulosis, and allergic angiitis (Figs. 11–10, 11–11).

Capillary-Endothelial Proliferation

This terminology is used to characterize cutaneous diseases showing an increase in capillaries and endothelial cells as seen in juvenile hemangioma, granuloma pyogenicum, stasis dermatitis, wound healing, granulation tissue, areas of granulomatous inflammation, and ulcers (Figs. 7–46A, 11–2B).

Vascular Slits

This term refers to clefts lined by spindle-shaped cells and these spaces are usually engorged with red blood cells. Vascular slits are not lined by recognizable endothelial cells. This change is a characteristic feature seen in Kaposi's sarcoma. Lesions showing prominent fibrosis such as stasis ulcer may exhibit cleft-like spaces formed by retraction of connective tissue fibers from spindle-shaped fibrocytes and this change can be confused with the vascular slits of Kaposi's sarcoma (Fig. 29–12).

Desmoplasia or Desmoplastic Reaction

Desmoplasia means the formation and development of fibrous tissue in increased amounts resulting in fibrosis, fibromatosis, or scar formation. Dermal fibrocytic proliferation is seen in wound healing, scars, stasis dermatitis, folliculitis keloidalis, cystic acne, perifolliculitis capitis, cutaneous granulomatous inflammation, basal cell carcinoma, nevoid basal cell carcinoma syndrome, epithelioma adenoides cysticum, solitary trichoepithelioma, and some metastatic skin neoplasms (Figs. 7–16, 7–46A).

Retraction Spaces

In basal cell carcinoma, islands and strands of proliferating atypical basal keratinocytes show empty spaces or cleft-like separation of tumor cells from the adjacent desmoplastic dermis. Retraction spaces are often considered as artifacts from tissue fixation and dehydration, but even so, this feature is an aid in distinguishing basal cell carcinoma from squamous cell carcinoma, adnexal carcinoma, epithelioma adenoides cysticum, solitary trichoepithelioma, trichofolliculoma, and pseudoepitheliomatous hyperplasia of a basal cell type. Basal cell carcinoma with adenoid cystic changes show empty halos about islands of tumor cells, but histochemical stains for acid mucosaccharides demonstrate chondroitin sulfate B in the retraction spaces (Figs. 23–32B, 23–33A).

Cartwheel Pattern

This pattern characterizes dermal fibrocytic proliferation in which streams of spindle-shaped fibroblasts extend radially from a central hub similar to the spokes of a wheel. This feature is seen in dermatofibrosareoma protuberans, although fibromatosis, dermatofibroma, fibroxanthosarcoma, some metastatic carcinomas, and a few other cutaneous diseases showing fibrocytic

proliferation may sometimes exhibit a cartwheel-like pattern (Figs. 28–10, 28–11).

Curlicue Pattern

A dermal fibrocytic proliferation of spindle-shaped cells which appear narrow, curled, and twisted about obliterated vascular lumina and pseudo-lumina is referred to as the curlicue pattern. This feature is seen in some dermatofibromas, particularly the sclerosing hemangioma and histiocytoma types. Curlicue formation may sometimes be confused with the cartwheel pattern and lead to an erroneous diagnosis of dermatofibrosarcoma protuberans (Fig. 28–9).

Granuloma of the Skin

Cutaneous granulomatous inflammation is defined as circumscribed subacute to chronic inflammation localized about one or more foci of irritation and attended by varying degrees of epidermal hyperplasia, capillary-endothelial proliferation, fibrosis, and necrosis. Epithelioid cells, multinucleated giant cells, Langhans' giant cells, and Touton giant cells may be present. Cutaneous granulomatous inflammation will often show a prominent infiltrate of plasma cells which in various stages of degeneration appear as homogeneous acidophilic Russell bodies. Russell bodies are not specific for rhinoscleroma, but their presence in large numbers represents a significant change in the disease (Figs. 7–16, 7–21).

Epithelioid Cells

Epithelioid cells are specialized histiocytes which appear epithelial-like. These cells are commonly seen in cutaneous granulomatous diseases (Figs. 7–73A, 13–11B).

Tubercle

A tubercle represents an accumulation of epithelioid cells. In tuberculosis cutis such as lupus vulgaris, the tubercle is typically composed of epithelioid cells and a few Langhans' giant cells, and is surrounded by a mantle of lymphocytes. In cutaneous sarcoidosis, the tubercle is of the "naked" type with less inflammation. A sarcoid type of tubercle can be seen in silica granuloma, beryllium granuloma, cactus granuloma, zirconium granuloma, tertiary syphilis, tuberculosis cutis, tuberculoid leprosy, deep mycoses, and other granulomatous diseases (Figs. 13–11, 13–12B).

Subcutaneous tissue

Panniculitis

In dermal pathology, panniculitis simply means inflammation of subcutaneous fat tissue. The inflammation may cause subcutaneous tissue degeneration with disappearance of lipocytes, and this alteration has been referred to as "wucher atrophy" or fat replacement atrophy. This change is seen in erythema induratum, erythema nodosum, Weber-Christian disease, lipogranulomatosis, necrobiosis lipoidica, sclerosing lipogranuloma, and other diseases involving subcutaneous fat (Figs. 11–22A, 14–10A).

Summary and Conclusions

Important cutaneous basic pathologic changes using appropriate terminology and workable definitions have been presented. To master dermal pathology, it is necessary to microscopically recognize and understand the various tissue alterations occurring in cutaneous diseases. In most instances, attaching significance to one or a combination of basic pathologic changes in skin biopsy tissue sections will allow for an objective diagnosis to be made or at least make possible a realistic microscopic differential. When skin sections are judged as showing nondiagnostic tissue changes, knowledgeable correlation of the microscopic and clinical features will usually result in the correct diagnosis.

INDEX OF SELECTED ILLUSTRATIONS FOR EACH DEFINITION

8–16, 9–4, 11–5, 11–18, 11–20, 13–1, 24–1A, 24–6A, 24–20, 24–28B, 24–29, 24–42.

Hypokeratosis. Figs. 7–3, 7–4A, 7–12A, 7–39, 7–65B, 7–74A, 7–81A, 11–5, 11–6, 11–27A, 24–45, 24–47A, 24–55A, 24–56A.

Hypopigmentation. Figs. 7–96A, 11–23.

Incontinence of Pigment. Fig. 11–31.

Intercellular Edema or Spongiosis. Figs. 1–8, 7–34A, 7–36A, 7–39, 7–59A, 7–60A, 7–62A, 7–63B, 7–64, 7–65, 7–67A, 7–70, 7–71A, 7–75A, 7–85A, 7–86A, 7–88A, 7–91A, 9–1, 9–10B, 11–4, 11–14, 11–18, 11–26, 13–1, 13–6A, 33–4B.

Interstitial Edema. Figs. 7–9A, 7–12, 7–39A, 7–44A, 7–60A, 7–64, 7–65B, 7–67A, 7–70, 7–71A, 7–81A, 7–88A, 7–108A, 8–2, 8–16, 9–1, 9–8, 9–9, 9–10B, 9–22B, 9–23B, 9–35, 9–36A, 9–37, 9–42, 9–46, 11–4, 11–14, 11–26, 35–4 to 35–6.

Intracellular Edema or Alteration Cavitaire. Figs. 7–35A, 7–35B, 7–36A, 7–62A, 7–64, 7–65, 7–86A, 9–1, 11–4, 11–14.

Karyorrhexis. Fig. 11–19B.

Liquefaction Degeneration or Hydropic Degeneration of Basal Cells. Figs. 7–39, 8–1 to 8–3, 8–7, 8–15, 8–16, 9–1, 9–37, 9–38, 9–40, 11–20, 11–25A, 11–26, 15–1, 24–4B.

Melanophage. Figs. 20–1, 20–2, 24–8, 24–62A.

Metachromasia. Fig. 35–7C.

Metaplasia. Fig. 23–30.

Microabscess. Figs. 7–40, 7–41A, 7–42, 7–62A, 7–67A, 9–28, 9–29, 31–8A, 31–8B, 31–10A.

Mucinous or Myxoid Degeneration. Figs. 7–32C, 7–32D, 7–43A, 8–9, 8–14, 11–13, 11–21, 22–28, 35–15, 35–16A to 35–16D, 35–17 to 35–19.

Necrobiosis. Figs. 7–43A, 16–1, 16–3, 16–4A, 16–5, 17–2 to 17–5, 18–2, 31–1.

Necrolysis or Necrolytic Changes. Figs. 8–1 to 8–13, 8–16, 8–17, 9–1.

Nesting or Theques of Cells. Figs. 5–15, 20–3, 20–5, 20–9, 20–10, 20–21, 20–22, 23–11B, 24–30, 24–66, 24–67, 24–68 to 24–72A, 24–73A, 27–2.

Panniculitis. Figs. 11–22A, 14–10A, 18–9A, 18–11 to 18–14A.

Papilloma. Figs. 23–4, 23–9, 23–10B, 23–17, 24–5, 24–13, 24–49, 24–70A.

Papillomatosis. Figs. 7–52A, 7–88A, 23–1, 23–4, 23–8, 23–9, 24–5A, 24–9A, 24–13A.

Parakeratosis. Figs. 7–16A, 7–21, 7–22A, 7–34B, 7–62, 7–74A, 7–75A, 7–81B, 7–83A, 7–85A, 7–85B, 7–87, 7–88A, 8–2, 8–5, 8–6, 8–7, 8–15, 8–16, 9–3, 9–6A, 9–10A, 9–12A, 10–1, 11–4, 11–20, 13–1, 13–6A, 14–3A, 23–20, 24–1A, 24–6A, 24–20, 24–21A, 24–22, 24–28B, 24–29, 24–32A, 24–42, 24–52, 24–67A, 29–7, 31–3A, 31–4B, 31–9A.

Peripheral Palisading. Figs. 16–1, 16–5, 17–3, 17–5, 23–32B, 23–33A, 28–2, 30–2A, 31–1.

Pigmentation or Pigment Deposition. Figs. 11–5 to 11–9, 11–27 to 11–29A, 11–30, 11–31, 33–1 to 33–5.

Pseudoepitheliomatous Hyperplasia. Figs. 7–87, 7–88A, 11–7, 17–8, 18–7A, 19–10, 25–1, 25–2, 28–19.

Pyknosis. Figs. 8–2, 8–3, 8–11, 9–37, 11–19A, 35–14B.

Reticular Degeneration. Figs. 7–35A, 7–35B, 7–36A, 7–62, 9–1, 9–6, 11–4, 11–18.

Retraction Spaces. Figs. 23–32B, 23–33A.

Saw-Toothing. Figs. 9–36, 9–41, 9–42.

Sclerosis. Figs. 11–23, 11–30, 11–31, 11–33, 24–48, 35–1, 35–2, 35–3A to 35–3C.

Squamous Eddy. Figs. 11–7, 23–11B, 24–67B.

Squamous Pearls. Figs. 24–14, 24–17, 24–24, 24–27, 27–2.

Superficial Crusting. Figs. 7–21, 7–34A, 7–35A, 10–4, 24–24A.

Thinning of Suprapapillary Epidermal Plates. Fig. 11–26A.

Tubercle. Figs. 13–11, 13–12B, 14–2, 14–3B, 14–3C, 14–4, 14–8, 14–10B, 14–12, 14–14, 15–1, 15–2 to 15–4, 15–6 to 15–8, 18–2, 18–3, 19–9.

Vacuolation. Figs. 7–89B, 7–108A, 8–2A, 8–3, 8–7, 8–11, 8–15, 9–4, 9–11, 9–13, 9–37, 9–38, 11–7, 11–14, 11–18, 11–19A, 23–3, 23–7, 24–5B, 24–6, 24–9B, 24–28B, 24–29 to 24–33, 24–35B, 24–36A, 24–40B, 24–42, 24–53, 24–55, 24–56, 24–57, 24–58, 24–59, 24–63, 24–65, 35–14B.

Vascular Ectasia. Figs. 7–41, 7–88A, 8–1, 8–6, 8–16, 9–9B, 9–24B, 11–6, 11–8B, 11–14, 11–17A, 11–19A, 11–30B, 11–31A, 13–14B, 23–16, 23–19, 24–3, 24–4A, 24–22, 24–45, 24–47A, 29–2, 29–3, 29–5 to 29–10.

Vascular Obliteration. Figs. 11–10, 11–11, 11–22, 11–25B, 11–30, 11–31A, 11–32, 16–2.

Vascular Slits. Fig. 29–12.

Vesicle or Bulla. Figs. 7–37A, 7–61, 7–65, 7–84A, 8–3 to 8–5, 8–11, 8–12, 8–17, 9–1 to 9–47, 11–4, 12–2B, 23–20, 24–19, 24–20, 35–4B.

Villi. Figs. 9–8, 9–9, 22–20 to 20–23, 23–22, 24–19.

REFERENCES

1. Allen, A. C. The Skin: A Clinicopathologic Treatise, 2nd ed. New York, Grune & Stratton, 1967, p. 79.
2. Lever, W. F. Histopathology of the Skin, 4th ed. Philadelphia, Lippincott, 1967, pp. 773–776.
3. Montgomery, H. Dermatopathology. New York, Harper and Row, 1967, vol. 1, pp. 3–8.
4. Leider, M., and Rosenblum, M. A Dictionary of Dermatological Words, Terms and Phrases. New York, McGraw-Hill, 1968.
5. Pinkus, H., and Mehregan, A. H. A Guide to Dermatohistopathology. New York, Appleton-Century-Crofts, 1969, pp. 70–86.

EXHIBIT F

COPY OF (ROUGIER ET AL., *J. PHARM. SCI.*, 76:451-454 (1987)

s

'76, 65, 1140.
976, 4, 395.
n. Biopharm. 1979,

armacol. 1984, 26,

985, 74, 388.
; Uno, T. J. Pharm.

Biopharm. 1980, 8,

gele, D. In Methods
oodcock, B.; Neu-
85–93.
82, 44, 1065.
. 1983, 7, 107.
.; Nakagawa, M.;

83, 45, 623.
ed and Controlled
I. R., Ed.; Marcel

77, 66, 178.
harm. 1978, 6, 79.
78, 6, 227.
4.
, 6, 227.
Systems; Finkel-
es: Forest Grove,

gy and Medicine;
109.
inetics; Blaisdell:

In Vivo Percutaneous Penetration of Some Organic Compounds Related to Anatomic Site in Humans: Predictive Assessment by the Stripping Method

ANDRÉ ROUGIER[x]*, CLAIRE LOTTE*, AND HOWARD I. MAIBACH‡

Received August 5, 1986, from the *Département de Biologie, Laboratoires de Recherche Fondamentale de L'OREAL, 1 Avenue Eugène Schueller, 93601 Aulnay sous bois, France, and the ‡Department of Dermatology, University of California, San Francisco, CA 94143. Accepted for publication April 7, 1987.

Abstract □ The effect of anatomic site on the in vivo relationship between the total penetration of four compounds and the amount of the compounds present in the stratum corneum at the end of application was studied in humans. For each anatomic site, 1000 nmol of ^{14}C-radiolabeled benzoic acid, benzoic acid sodium salt, caffeine, or acetylsalicylic acid was applied to 1-cm^2 area of skin of male Caucasian patients aged 28 ± 2 years (groups of 6–8). For each molecule and each site, a first application on the right-hand side of the body allowed total absorption to be determined by measuring the amount excreted in the urine. A second application, performed 48 h later on the contralateral site, enabled the total amount of substance present in the stratum corneum at the end of application (30 min) to be assessed after cellophane-tape stripping of the treated area. The results showed that skin permeability varied substantially, depending both on the physicochemical nature of the molecule and on the anatomical location. In general, the rank order in skin permeability of the studied areas appears to be as follows: arm ≦ abdomen < postauricular < forehead. Whatever the compound applied, the forehead was ~2 times as permeable as the arm or abdomen. Independent of the origin of the differences in permeability observed among sites, there exists a linear correlation ($r = 0.97$, $p < 0.001$) between the amounts of substance present in the stratum corneum at the end of application (30 min) and the total amounts which penetrated within a 4-d period. The stripping method can therefore be used to make predictions of the total penetration of different chemicals, whatever the anatomic site, by simply measuring the quantities present in the stratum corneum at the end of the application.

The rate of absorption of molecules depends on application conditions which may partly explain the wide variations reported for the same substance. For example, the animal species,[1–3] the vehicle used,[1,4,5] the dose applied,[3,6,7] and the contact time[1,8,9] are factors which considerably affect the absorption rate of a compound.

In previous studies on rat[10] and humans,[3] it was shown that the total quantity of substance which penetrated over a 4-d period could be determined from the quantity present in the stratum corneum at the end of the application (30 min), with a linear correlation linking these two parameters. The predictive aspect of this new method of measuring percutaneous penetration was independent of the factors mentioned above that affect the absorption.[3,5,9,10]

Among other factors which might modify percutaneous absorption, both in vitro[11] and in vivo,[8,12–15] the anatomical location is of great importance, even if the connection between the differences observed, the structure of the skin, and the physicochemical nature of the applied molecule remain obscure.

This study ascertains whether, by use of the stripping method in humans, it is possible to predict the rate of absorption of a compound, whatever the anatomic area exposed.

Experimental Section

The percutaneous absorption of four radiolabeled compounds obtained from New England Nuclear [acetylsalicylic acid (carboxyl-^{14}C), specific activity 60 mCi/mmol, purity > 97%; benzoic acid (ring-^{14}C), specific activity 45 mCi/mmol, purity > 98%; caffeine (1-methyl-^{14}C), specific activity 55 mCi/mmol, purity > 97%; benzoic acid sodium salt (ring-^{14}C), specific activity 45 mCi/mmol, purity > 98%] was measured on four body sites (forehead, postauricular, upper outer arm, abdomen). For each molecule and each location, 6 to 8 male, Caucasian, informed volunteers, aged 28 ± 2 years, were studied.

On each volunteer, two strictly identical applications were performed at an interval of 48 h. The first application, designed to measure the total penetration of the molecule involved, was made on the right-hand side of the body. The second, on the contralateral site, was used to determine the amount of substance present in the stratum corneum at the end of application.

Application Conditions—One thousand nanomoles of each molecule, with a specific activity of 10^{-3} μCi/nmol, were applied to a 1-cm^2 area of skin in 20 μL of a vehicle, the composition of which (Table I) was chosen according to the solubility of each compound. Triton X-100 (Marke Rohm and Haas), added as a surfactant, promoted even spreading of the vehicle over the treated area. For each anatomic site, the treated area was delimited by an open circular cell that was fixed by silicone glue to prevent chemical loss. After 30 min of contact, the excessive substance in the dosed area was quickly removed by washing twice (2 × 300 μL) with a 95:5 ethanol:water mixture, rinsing twice (2 × 300 μL) with distilled water, and then lightly dried with a cotton ball.

Percutaneous Absorption Measurements—The daily levels of urinary excretion of the molecules studied, given either percutaneously or intravenously in humans and in animals, are described clearly in the literature. Therefore, it was possible to deduce the total amounts which penetrated over a 4-d period from those excreted in the urine during the first 24 h. This procedure eliminated the need to measure percutaneous absorption after correction by parenteral injection, which for obvious reasons is always difficult to perform in humans, particularly when radiolabeled compounds are used. For example, in the rat, the amount of benzoic acid excreted in the urine during the first 24 h of the experiment is 75% of the quantity administered when injected intravenously,[16] and an average of 77% when given topically.[3,9,10] In humans, after topical application, the first 24-h urine sample contains 75% of the benzoic acid penetrating the skin over a 4-d period.[3] Regarding acetylsalicylic acid given percutaneously, previous studies showed that the first 24-h urine sample contains 45% of the total amount penetrating over a 4-d period in the rat[9,10] and 31% in humans.[17] It was also demonstrated that the quantities of caffeine found in the first 24-h urine sample were 48 and 49%, respectively, of the total quantity penetrating in 4 d when the molecule was given topically in the rat[10] and in humans.[17] On the basis of these findings, it was possible to deduce the total quantitites of benzoic acid, acetylsalicylic acid, and caffeine penetrating during a 4-d period, after a liquid scintillation counting of the urine collected during the first 24-h period. The quantities of benzoic acid, acetylsalicylic acid, and caffeine penetrating over a 4-d period were 75, 31, and 50%, respectively.

0022-3549/87/0600-0451$01.00/0

Table I—Percutaneous Absorption of the Tested Molecules According to Anatomic Site[a]

Anatomic Site	Amount in Urine Samples after 24 h (A), nmol/cm²	Total Amount Penetrated within 4 d (B), nmol/cm²	Amount in the Stratum Corneum 30 min after Application, nmol/cm²	Predicted Penetration within 4 d, nmol/cm²
Benzoic Acid Sodium Salt[b]				
Arm (upper, outer) (n = 6)	3.02 (0.34)	4.02 (0.45)[c]	2.83 (0.58)	4.67 (1.07)
Abdomen (n = 6)	5.73 (0.54)	7.65 (0.72)[c]	4.04 (0.98)	6.88 (1.80)
Post Auricular (n = 6)	7.54 (0.62)	10.06 (0.82)[c]	6.29 (0.93)	11.02 (1.72)
Forehead (n = 8)	9.31 (1.76)	12.32 (2.30)[c]	5.94 (0.99)	10.34 (1.81)
Caffeine[d]				
Arm (upper, outer) (n = 7)	6.04 (0.92)	12.09 (1.84)[e]	6.75 (0.84)	11.83 (1.53)
Abdomen (n = 6)	3.76 (0.67)	7.53 (1.34)[e]	4.31 (0.60)	7.36 (1.11)
Post Auricular (n = 7)	5.87 (0.52)	11.72 (1.05)[e]	7.46 (1.24)	13.13 (2.26)
Forehead (n = 6)	11.17 (1.20)	22.35 (2.39)[e]	11.60 (1.52)	20.71 (2.79)
Benzoic Acid[f]				
Arm (upper, outer) (n = 8)	6.87 (0.75)	9.15 (1.01)[g]	5.70 (0.58)	9.90 (1.00)
Abdomen (n = 7)	10.88 (1.23)	14.51 (1.64)[g]	7.89 (1.12)	13.92 (1.97)
Post Auricular (n = 8)	16.87 (3.85)	22.49 (5.14)[g]	10.53 (0.63)	18.75 (1.15)
Forehead (n = 7)	20.30 (2.39)	26.80 (3.19)[g]	13.20 (2.70)	23.63 (4.79)
Acetyl Salicylic Acid[f]				
Arm (upper, outer) (n = 7)	5.27 (0.18)	17.00 (0.37)[h]	11.99 (1.34)	21.42 (2.45)
Abdomen (n = 6)	5.34 (1.03)	17.20 (3.35)[h]	9.98 (1.98)	17.74 (3.62)
Post Auricular (n = 6)	11.04 (2.50)	29.2 (5.37)[h]	14.56 (1.30)	26.10 (2.38)
Forehead (n = 6)	10.89 (1.02)	35.14 (3.29)[h]	21.97 (4.29)	40.20 (7.75)

[a] Values are expressed as mean ± SD in parentheses. [b] Vehicle: ethyleneglycol:Triton X-100 (90:10). [c] Calculated from urinary excretion: B = A/0.75. [d] Vehicle: (ethyleneglycol:Triton X-100): H_2O (50:50). [e] Calculated from urinary excretion: B = A/0.5. [f] Vehicle: ethyleneglycol:Triton X-100: (90:10). [g] Calculated from urinary excretion: B = A/0.75. [h] Calculated from urinary excretion: B = A/0.31.

We were unable to find any references on the kinetics of the excretion of sodium benzoate in the urine when given topically or intravenously. However, in view of the similar structures of sodium benzoate and benzoic acid, we have assumed that the kinetics of excretion of these two molecules in the urine are comparable.

Tape Strippings—At the end of the second application (30 min) and after washing, the stratum corneum of the treated area was removed by 15 successive strippings (3M adhesive tape). For each molecule and each anatomic site, the radioactivity present in the horny layer was measured after complete digestion of the keratinic material by Soluene 350 (United Technology Packard, USA), addition of Dimilume 30 (United Technology Packard, USA), and liquid scintillation counting (Packard 460 C, Packard Instruments, USA).

Results

The amount of molecule present in the 24-h urine sample, and the total amount absorbed in 4 d (calculated from the amount in the 24-h urine sample), for each anatomic site are shown in Table I. There are appreciable differences in permeability among sites. To make comparisons easier, Figure 1 expresses the permeability of each area to the various molecules in relation to that of the arm to benzoic acid sodium salt. This has the advantage of simultaneously showing differences in permeability due to the physicochemical properties of the molecules and to the applied area.

Figure 2 presents the relationship between total percutaneous absorption values of each of the molecules studied and their amounts in the stratum corneum at the end of application time (30 min) for each patient, separately and combining the findings for all the sites involved ($n = 107$, $r = 0.70$, $p < 0.001$). The confidence limits represented constituted a risk level of 5%.

Figure 3 shows the linear relation ($r = 0.97$, $p < 0.001$), for each anatomic site and each compound, between the mean values of the total penetration and the mean values of the amounts present in the horny layer at the end of application (30 min; Table I). The correlation line obtained between these two parameters can thus be used to predict the total amounts likely to penetrate during a 4-d period, by simply measuring the amounts of chemical present in the stratum corneum at the end of application. As shown in Table I, there exists a high level of agreement between the mean values of penetration measured and those predicted, whatever the site involved and the compound applied.

Discussion

Although all authors agree on the importance of anatomic location in percutaneous absorption, the literature contains minimal documentation. General reviews[11,18,19] often give contradictory explanations for the differences in permeability observed from one site to another. Our results (Table I) show that there exists appreciable differences in skin permeability according to both the physicochemical nature of the molecule applied and the anatomic site treated.

Figure 1 simultaneously shows the effect of these parameters, with the penetration values expressed in relation to that of benzoic acid sodium salt on the arm. The rank order in skin permeability of the areas studied appears to be as follows: arm ≦ abdomen < postauricular < forehead. Whatever the molecule applied, the forehead is ~2 times as permeable as the arm or the abdomen. This average ratio agrees well with those reported for the same areas with other molecules such as hydrocortisone,[13] and parathion and malathion.[14] A possible explanation of the higher penetration in areas such as the forehead, where there are more sebaceous glands, could be that absorption occurs through the follicles rather than through the epidermis. However, how do we reconcile the great disproportion (factor of 50 to 100) existing between the number of sebaceous glands of these two sites,[20,21] and the relatively small difference (factor of 2 to 3) observed in skin permeability (Table I, Figure 1).

Because of the density of active sebaceous glands, the

forehead is the richest of all the sites in term of sebum which forms a discontinuous film on the surface of the skin, between 0.4 and 4 μm thick.[22] Questions to be considered are the extent of interaction between the physicochemical properties of the molecule applied and this film, and the effects that this first contact may have on absorption. In the past, the presence of sebum was believed to reduce absorption of hydrophilic substances.[23] This theory has since been disproved.[24] Removing the lipidic film from the surface or artificially increasing the thickness has no effect on transepidermal water loss,[25,26] which is another indicator of skin permeability. Furthermore, our results show (Table I, Figure 1) that the same ratio exists (factor of 2) between the permeability levels of areas such as the forehead, which is rich in sebum, and the arm, which has none, to molecules with totally different lipid solubility, such as benzoic acid and its sodium salt. It is worth noting that, in absolute values and for all the sites studied, the penetration level of benzoic acid is ~2 times higher than that of benzoic acid sodium salt (Table I). Since these two molecules are practically identical in structure, this result suggests the importance of solubility in absorption phenomena, particularly in the interaction between the molecule, the vehicle, and the horny layer. Finally, as in previous studies,[27] it appears that salts are not absorbed as well as their corresponding acids.

Among numerous applications of studies on the relationship existing between skin permeability and anatomic site, considerable attention has been given to finding a favorable "window" for transdermal treatment of systemic diseases. For various reasons, the postauricular area is used most often for scopolamine transdermal drug delivery systems.[28,29] As the data in Table I and Figure 1 show, this area has a high level of permeability, whatever the molecule applied. Apart from caffeine, it is statistically higher than that of the arm or abdomen and often similar or equal to that of the forehead. According to Taskovitch and Shaw,[30] the closeness of the capillaries to the surface of the skin, due to pronounced anchorage of the dermal papilla in the epidermis, may promote resorption of substances and give the postauricular area its good permeability.

Previous studies[10] have shown that the total amount of a substance likely to penetrate over a 4-d period can be deduced by simply measuring the amounts present in the stratum corneum after a 30-min application. In addition, the strict correlation between these two parameters, verified in two such different species as the human and the hairless rat,[3] has been shown to be unaffected by the physicochemical nature of the compound studied,[9,10] the dose applied,[3] the application time,[9] and the vehicle used.[5]

Table I gives the amount of each molecule tested that is found in the stratum corneum at the end of the application. These quantities, in fact, correspond to the affinity of each molecule for the horny layer and can be considered as an indication of their partitioning between vehicle and stratum corneum. As Figure 3 shows, the relation between the amount of substance present in the stratum corneum at the end of the application (30 min) and the total amount ab-

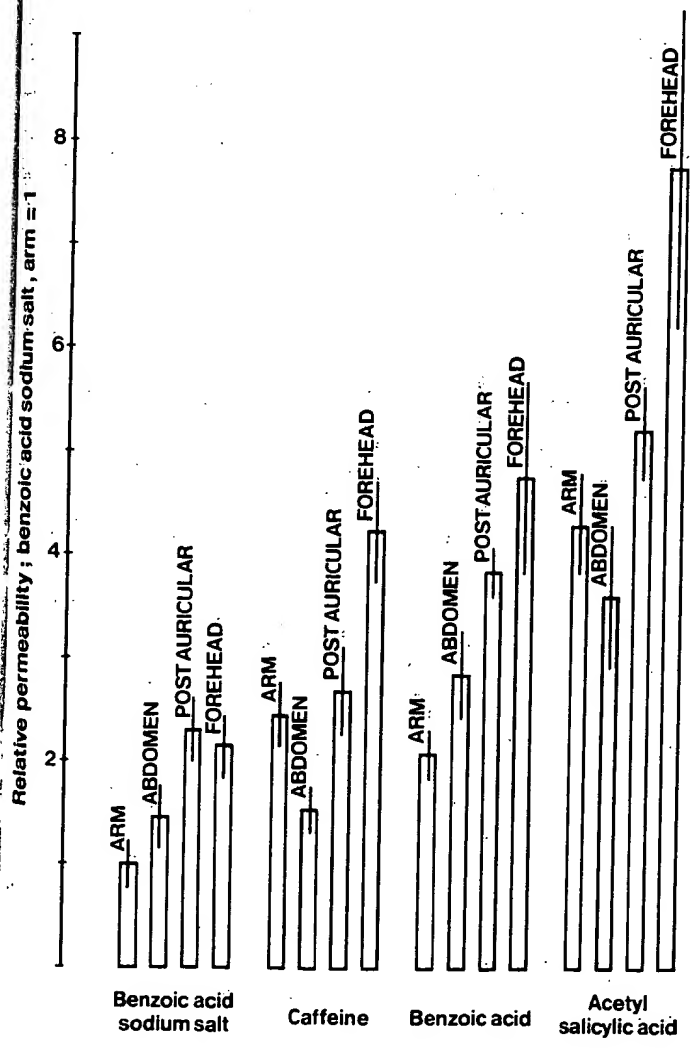

Figure 1—*Total penetration of the tested molecules according to anatomic site (the values are expressed relative to that of benzoic acid sodium salt applied on the arm).*

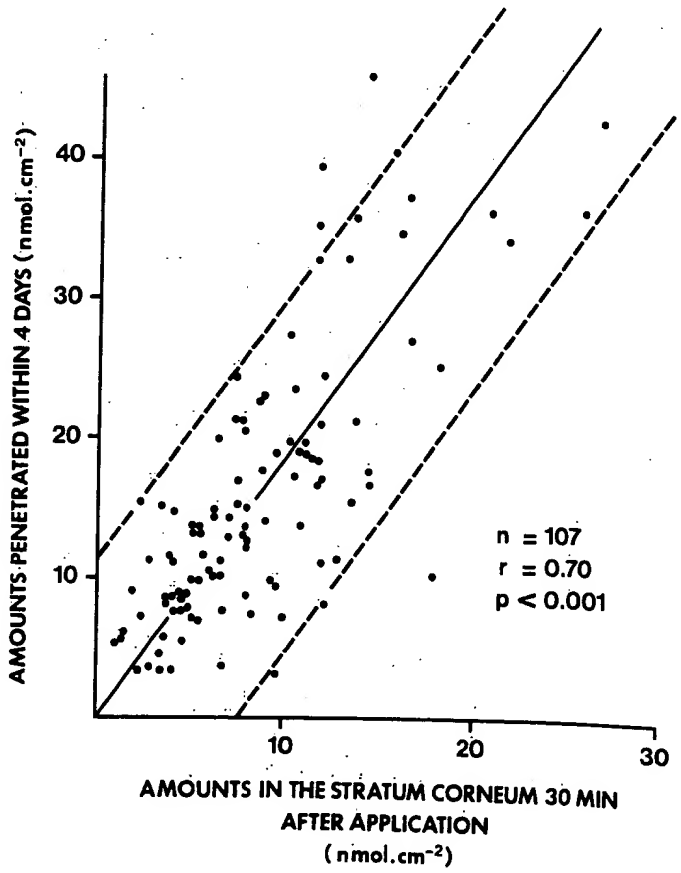

Figure 2—*Correlation between the penetration levels of the molecules within 96 h and their concentration in the stratum corneum after 30 min of application; for each patient individually and independent of the molecule applied and the anatomic site involved.*

sorbed within 4 d is confirmed in the human, in the case of application to different anatomical sites. In order to standardize the proposed method, the correlation curve in Figure 3, with the equation $y = 1.83x - 0.52$, corresponds to that first established in the human with increasing doses of benzoic acid.[3] It should be noted that the experimental points obtained in the present study are close to this curve and correlate with a coefficient of variation of 0.97 and $p < 0.001$. The confidence limits represented constituted a risk of 5%.

As a consequence, by simply measuring the quantity (x) of a substance present in the stratum corneum at the end of the application (30 min), it is possible to predict the total quantity absorbed over a 4-d period. Table I shows that, independent of the physicochemical nature of the penetrant and whatever the factors involved in differences of permeability between sites, the total penetration values measured correspond closely to those predicted after 30 min of contact by the stripping method.

For technical convenience, radiolabeled compounds were used in this study. However, because of the relatively large amounts of substance present in the horny layer at the end of application, it should be possible, with the stripping method, to measure percutaneous absorption in humans by appropriate nonradioactive analytical techniques. However, in cases where it is nevertheless essential to use radiolabeled substances, this method makes it possible both to substantially reduce the level of radioactivity administered and to limit contact time.

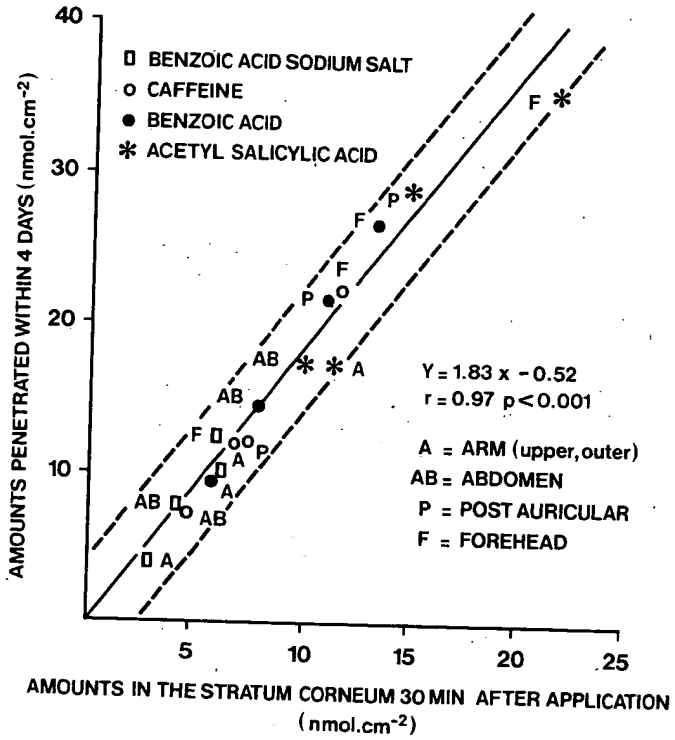

Figure 3—*Correlation between the mean values of total penetration within 96 h and the mean values of the amounts present in the stratum corneum after 30 min of application for each compound and each anatomic site.*

References and Notes

1. Tregear, R. T. In *Progress in Biological Sciences in Relation to Dermatology*; Rook, A.; Champion, R. H., Eds.; Cambridge University: 1964, pp 275–281.
2. Winkelmann, R. K. *Br. J. Dermatol.* 1969, *81*, 11–22.
3. Dupuis, D.; Rougier, A.; Roguet, R.; Lotte, C.; Kalopissis, G. *J. Invest. Dermatol.* 1984, *82*, 353–356.
4. Poulsen, B. J. In *Drug Design*, vol. IV; Ariens, E. J., Ed.; New York Academic: 1973; pp 149–190.
5. Dupuis, D.; Rougier, A.; Roguet, R.; Lotte, C. *Br. J. Dermatol.* 1986, *115*, 233–238.
6. Maibach, H. I.; Feldmann, R. J. *J. Invest. Dermatol.* 1969, *52*, 382.
7. Wester, R. C.; Maibach, H. I. In *Dermatology vol. 6: Percutaneous Absorption—Mechanism—Methodology—Drug Delivery*; Bronaugh, R. L.; Maibach, H. I., Eds.; Marcel Dekker: New York and Basel, 1985; pp 347–361.
8. Wester, R. C.; Maibach, H. I. *Drug Metab. Rev.* 1983, *14*, 169–205.
9. Rougier, A.; Dupuis, D.; Lotte, C.; Roguet, R. *J. Invest. Dermatol.* 1985, *84*, 66–68.
10. Rougier, A.; Dupuis, D.; Lotte, C.; Roguet, R.; Schaefer, H. *J. Invest. Dermatol.* 1983, *81*, 275–278.
11. Scheuplein, R. J. In *Physiology and Pathophysiology of the Skin*; Jarret, P., Ed.; Academic Press: New York, 1979; pp 1731–1752.
12. Britz, M. B.; Maibach, H. I.; Anjo, D. M. *Arch. Derm. Res.* 1980, *267*, 313–316.
13. Feldmann, R. J.; Maibach, H. I. *J. Invest. Dermatol.* 1967, *48*, 181–183.
14. Maibach, H. I.; Feldmann, R. J.; Milby, T. H.; Serat, W. F. *Arch. Environ. Health* 1971, *23*, 208–211.
15. Wester, R. C.; Maibach, H. I.; Bucks, D. A. Aufrere, M. B. *J. Toxicol. Environ. Health* 1984, *14*, 759–762.
16. Bronaugh, R. L.; Stewart, R. F.; Congdon, E. R.; Giles, A. L. *Toxicol. Appl. Pharmacol.* 1982, *62*, 474–480.
17. Feldmann, R. J.; Maibach, H. I. *J. Invest. Dermatol.* 1970, *54*, 399–404.
18. Barry, B. W. In *Drugs and Pharmaceutical Sciences*, Vol. 18; Swarbrick, J., Ed.; M. Dekker: New York and Basel, 1983.
19. Idson, B. *J. Pharm. Sci.* 1975, *64*, 901–924.
20. Benfenati, A.; Brillanti, F. *Arch. Ital. Dermatol.* 1939, *15*, 33–42.
21. Szabo, G. In *The Biology of Hair Growth*; Montagna, W.; Ellis, R. A., Eds.; New York Academic: 1958; pp 33–38.
22. Kligmann, A. M. *Drug Dev. Indust. Pharm.* 1983, *9*, 521–560.
23. Calvery, H. O.; Draize, J. H.; Lang, E. P. *Physiol. Rev.* 1946, *26*, 495–540.
24. Blank, I. H.; Gould, E. *J. Invest. Dermatol.* 1961, *37*, 311–315.
25. Burch, G. E.; De Pasquale, N. P. *Hot Climates: Man and His Heart*; Springfield, IL, 1962.
26. Kligman, A. M. *J. Dermatol.* 1983, *75*, 307–319.
27. Malkinson, F. D.; Rothman, S. In *Handbuch der Haut und Geschlecht Skrauberten Normale und Pathologische der Haut*, Vol. 1, Part 1; Erganzungswerk Bd 1/3; Marchionini, A.; Spier, H. W., Eds.; Springer: Berlin, Gottingen, Heidelberg, 1963; pp 90–156.
28. Shaw, J. E.; Chandrasekaran, S. K.; Micharls, A. S.; Taskovitch, L. In *Animal Models in Human Dermatology*; Maibach, H. I., Ed.; Churchill Livingstone: Edinburgh and London, 1975; pp 138–146.
29. Shaw, J. E.; Chandrasekaran, S. K.; Campbell, P. S.; Schmitt, L. G. In *Cutaneous Toxicity*; Drill, V. A.; Lazar, P., Eds.; New York Academic: 1977; pp 83–94.
30. Taskovitch, L.; Shaw, J. E. *J. Invest. Dermatol.* 1978, *70*, 217.

Acknowledgments

The authors would like to thank A. M. Cabaillot and J. McMaster for their excellent technical assistance.

EXHIBIT G

COPY OF HOLLERAN ET AL., *J. LIPID RES.*, 32:1151-58 (1991)

Regulation of epidermal sphingolipid synthesis by permeability barrier function

Walter M. Holleran, Kenneth R. Feingold, Man Mao-Qiang, Wen N. Gao, Jane M. Lee, and Peter M. Elias

Departments of Dermatology and Medicine, University of California School of Medicine, and Dermatology Service and Metabolism Section, Veterans Administration Medical Center, San Francisco, CA 94121

Abstract A mixture of sphingolipids, cholesterol, and free fatty acids forms the intercellular membrane bilayers of the stratum corneum which are presumed to regulate epidermal barrier function. Prior studies have shown that both cholesterol and fatty acid synthesis are rapidly regulated by epidermal barrier requirements. In contrast, the importance of sphingolipids in barrier function has not been directly demonstrated. Here, we have assessed both sphingolipid synthesis by $[^3H]H_2O$ incorporation and serine palmitoyl transferase (SPT) activity in relation to modulations in barrier function. Incorporation of $[^3H]H_2O$ into sphingolipids increased after barrier disruption with acetone, with maximal increase (170%) occurring 5–7 h after treatment ($P < 0.005$). As barrier function returned to normal over 24 h, incorporation of tritium into sphingolipids normalized. SPT activity also increased after barrier disruption, peaking at 6 h (150%) ($P < 0.05$), and returning towards normal by 24 h. Artificial restoration of the barrier with a water vapor-impermeable membrane prevented the increases in both $[^3H]H_2O$ incorporation into sphingolipids and enzyme activity. Finally, SPT activity was increased in two other models of barrier dysfunction, cellophane tape-stripping and essential fatty acid deficiency. Occlusion normalized SPT activity in both of these models as well. These studies: *a*) demonstrate a distinctive, delayed increase in epidermal sphingolipid synthesis in response to barrier requirements that contrasts with the immediate responses of cholesterol and fatty acid synthesis; and *b*) suggest that sphingolipids are important for the maintenance of the epidermal permeability barrier.—**Holleran, W. M., K. R. Feingold, M. Mao-Qiang, W. N. Gao, J. M. Lee, and P. M. Elias.** Regulation of epidermal sphingolipid synthesis by permeability barrier function. *J. Lipid Res.* 1991. 32: 1151–1158.

Supplementary key words sphingolipids • serine-palmitoyl transferase • epidermal barrier function

Cornification of the epidermis of terrestrial mammals is accompanied both by sequestration of lipids to intercellular domains (1, 2), as well as profound alterations in lipid biochemical composition (3). Toward the outer cell layers of the epidermis, phospholipid content diminishes and a relatively nonpolar mixture of lipids emerges that is enriched in cholesterol, free fatty acids, and sphingolipids (4–7). These species are organized into a system of parallel membrane bilayers that is presumed to mediate the cutaneous permeability barrier (1, 2).

Recent metabolic studies have demonstrated the importance of both cholesterol and fatty acids for barrier homeostasis (8–12). However, the evidence to date for a role of sphingolipids in epidermal barrier function has been largely indirect and includes the following: first, a family of sphingolipids represents the predominant lipid species on a weight basis (35–40%) in the stratum corneum intercellular domains (5–7, 13). Second, these sphingolipids are also the principal repository for the highly saturated, very-long chain (C22:0–C26:0) fatty acids among esterified stratum corneum species (7). And, in marine cetaceans, the very long-chain, N-acyl fatty acids are replaced by shorter chain species (14), which may reflect the less stringent barrier requirements of the marine environment. Third, the majority of epidermal linoleic acid, an essential fatty acid known to be required for cutaneous barrier function (15–17), is esterfied to ceramide at the ω-hydroxy terminus of the N-acyl fatty acid (18–20). Decreased linoleic acid content in essential fatty acid deficiency leads to an abnormal permeability barrier (21, 22), which has been attributed to substitution of oleic for linoleic acid in the epidermal sphingolipids (23). Fourth, only polar organic solvents that remove sphingolipids as well as neutral lipids from the stratum corneum are capable of significant abrogation of the permeability barrier (24). Finally, topical applications of certain natural and synthetic ceramides correct the abnormal water-retaining properties of solvent- or detergent-extracted stratum corneum (25).

Abbreviations: SPT, serine-palmitoyl transferase; CH, cholesterol; FA, fatty acid; SPL, sphingolipid; TEWL, transepidermal water loss; EFAD, essential fatty acid deficiency; HPTLC, high performance thin-layer chromatography; 3-KDS, 3-ketodihydrosphinganine.

We have recently shown that both cultured human keratinocytes, as well as murine epidermis, are highly enriched in serine palmitoyl transferase (EC2.3.1.50; SPT) (26), the rate-limiting enzyme of sphingolipid base synthesis (27, 28). In order to assess the role of sphingolipids in the barrier, we measured both epidermal sphingolipid synthesis and SPT activity in animals undergoing various types of experimental barrier perturbation. We describe here elevations of both sphingolipid synthesis and SPT activity after acute perturbations of the permeability barrier. Moreover, both enzyme activity and synthesis were normalized when the barrier was artificially restored by occlusion, providing further evidence that sphingolipid synthesis is regulated by barrier requirements. Finally, these modulations in sphingolipid synthesis and SPT activity are different from those displayed by cholesterol (8, 12) and fatty acid (10) synthesis after barrier perturbation.

MATERIALS AND METHODS

Materials

Reagent grade organic solvents, pyridoxal phosphate, dithiothreitol, palmitoyl CoA, and sphingosine base were obtained from Sigma Chemical Co. (St. Louis, MO). HEPES buffer was purchased from Fisher Scientific (Santa Clara, CA); [^{3}H]H_2O (sp act 0.1 Ci/ml) and [3-^{3}H]L-serine (sp act 30 Ci/mmol) were obtained from Amersham (Arlington Heights, IL). High performance thin-layer chromatography (HPTLC) plates (silica gel 60) were obtained from Merck (Damstadt, FRG) (lot #5641). Protein reagent and bovine serum albumin standards were obtained from Bio-Rad (Richmond, CA).

Animals

Male hairless mice (Hr/Hr) between 4 and 12 weeks of age were purchased from Jackson or Simonsen Laboratories (Bar Harbour, ME and Gilroy, CA). They were fed Purina mouse diet and water ad libitum. For the essential fatty acid deficiency (EFAD) studies, mice were maintained on an EFAD diet (17) for 7–8 weeks until transepidermal water loss levels exceeded 1.0 mg/cm^2 per h.

Experimental design

Disruption of the permeability barrier was achieved by unilateral treatment of one flank of each animal with absolute acetone, as described previously (8, 10, 24, 29). Control animals were treated with 0.9% sodium chloride alone. Transepidermal water loss (TEWL) rates were measured with a Meeco^R electrolytic moisture analyzer (9, 10, 29), recorded in parts per million/0.5 cm^2 per h over background, and converted to mg H_2O/cm^2 per h according to the formula: $J = 6(18P/22.4A) \times 10^{-3}$; (P = increase over background, A = area of skin). To assess directly the effects of occlusion, which instantly lowers TEWL rates to zero, groups of acetone-treated tape-stripped, and EFAD animals were immediately covered with a tight-fitting, water-impermeable membrane (one finger of a Latex^R glove) (9, 10, 29). The wrap was removed just prior to excision of the whole skin samples for the biochemical studies described below.

Lipid incorporation studies

Approximately 8 cm^2 on one flank of each hairless mouse was gently swabbed with acetone-soaked cotton balls until TEWL readings exceeded 4.0 mg/cm^2 per h, measured over at least two separate sites. Animals were injected intraperitoneally with [^{3}H]H_2O (20 mCi/0.2 ml) at various time points after acetone treatment (1, 5, 10, and 22 h). Two hours after injection, blood samples were taken and the animals were killed. Whole skin was excised from each flank (acetone-treated vs. untreated sides), heated to 60°C for 60 sec, and the epidermis was separated from the dermis by gentle scraping (12). Samples were blotted dry, weighed, minced, immediately placed into screw-cap glass test tubes containing Bligh-Dyer solution (30), and total lipid extracts were obtained, as described previously (6). The lipid components then were separated by HPTLC using the following solvent sequence: *1*) chloroform–methanol–water 90:10:1 (by volume); *2*) petroleum ether–diethylether–acetic acid 70:50:1 (by volume); and *3*) chloroform–methanol–water–acetic acid 60:35:4.5:0.5 (by volume) to approximately 15 cm. Lipids were visualized by Woods light fluorescence after staining with 8-anilino-1-naphthalene sulfonic acid (ANS) (7), and identified by co-chromatography against known standards. The lipid spots, were scraped into scintillation vials and counted by liquid scintillation spectrometry. Total incorporation into sphingolipids was obtained by combining the ceramide, glycosphingolipid, sphingomyelin, and sphingosine base fractions. Using the specific activity of [^{3}H]H_2O in serum samples from each animal, results were expressed as μmoles incorporated per 2 h per mg of epidermal wet weight, as described previously (8–10, 31).

Microsomal isolation

Prior to assessment of SPT activity, microsomes were prepared from murine epidermis at various time points after barrier disruption as described previously (12). Briefly, whole skin was excised, incubated at 37°C for 45 min in phosphate-buffered saline (calcium/magnesium-free) containing 10 mM EDTA. The epidermis was peeled off the dermis with a scalpel blade, weighed, minced into small pieces (< 1 mm^3), and stored in small plastic tubes overnight at − 70°C. Samples then were thawed on ice, and five volumes of homogenization buffer were added (HEPES 50 mM, pH 7.4, containing 10 mM EDTA, 5

TABLE 1. Tritiated water incorporation into sphingolipids in acetone-treated versus untreated flanks

Time after Acetone Treatment	Synthesis Rate[a] Treated Side (Right)	Synthesis Rate[a] Untreated Side (Left)	Significance[b] (P)	Ratio[c] (R/L)
	μmol/mg/2 h			
Untreated	2.92 ± 0.44 (n = 7)	2.86 ± 0.42 (n = 7)	NS	1.0 ± 0.1
1–3 h	2.83 ± 0.40 (n = 6)	2.57 ± 0.29 (n = 6)	NS	1.2 ± 0.2
5–7 h	4.59 ± 0.38 (n = 7)	2.85 ± 0.25 (n = 7)	<0.005	1.7 ± 0.2
12–14 h	3.10 ± 0.35 (n = 5)	2.18 ± 0.21 (n = 5)	<0.005	1.4 ± 0.1
22–24 h	3.37 ± 0.28 (n = 5)	2.77 ± 0.19 (n = 5)	<0.05	1.2 ± 0.2

[a]Mean ± SEM (n).
[b]Determined by paired *t*-analysis, two-tailed.
[c]Mean (± SEM) of ratios for individual animals.

mM DTT, and 0.25 M sucrose). Cell homogenates were prepared using a Polytron PCU2 tissue homogenizer (Kinematica GmbH, Lucerne, Switzerland) followed by sonication using a Fisher Sonic Dismembranator (Model 300, Artec Systems Corporation, Farmingdale, NY), as described previously (12). Differential centrifugation (4°C) was performed, and the microsomal pellet (100,000 *g*) was resuspended in storage buffer containing 50 mM HEPES (pH 7.4), 5 mM EDTA, 5 mM DTT, and 20% glycerol (v/v) using a Dounce homogenizer, and stored at −70°C until use. No loss of enzyme activity was observed upon freezing or subsequent thawing; activity was stable for over 6 months at −70°C. In experiments with large numbers of tissue samples (n > 10), brief sonication was used to re-solubilize microsomal pellets. The enzyme activity for each experiment was related to a parallel normal control group. The protein content of various subcellular fractions was determined by the Bradford procedure (32) using bovine serum albumin as standard. DNA content was determined using the method of LaBarca and Paigen (33).

Serine palmitoyl transferase (SPT) assay

Our assay for SPT activity was modified from the method of Williams, Wang, and Merrill (28), as recently described (26). Briefly, the assay buffer contained 100 mM HEPES, pH 8.3, 5.0 mM DTT, and 2.5 mM EDTA, while the reaction mixture contained 50 μM pyridoxal phosphate, 150 mM palmitoyl-coenzyme A, 1.0 mM [^{3}H]L-serine (sp act 45 to 50,000 dpm/nmol), and 50 to 100 μg of microsomal protein in 0.1 ml total assay volume. The assay mixture (protein, buffer, and pyridoxal phosphate) was preincubated for 10 min (37°C), and the assay was initiated by simultaneous addition of palmitoyl CoA and [^{3}H]L-serine, incubated at 37°C for 10 min, and terminated by the addition of 0.2 ml of 0.5 N NH_4OH. The reaction product, 3-ketodihydrosphinganine (3KDS), was isolated as described previously (26) and counted by liquid scintillation spectrometry. Enzyme specific activity was expressed as pmoles of 3KDS formed per minute per mg of microsomal protein. Total SPT activity was obtained by multiplying the specific activity by the total protein (total pmol 3KDS formed/min).

Statistical analysis

Statistical evaluation of data was performed using either a two-tailed Student's *t*-test or paired *t*-test.

RESULTS

Sphingolipid synthesis

To determine whether epidermal barrier requirements regulate sphingolipid synthesis, we first examined the incorporation of [^{3}H]H_2O into these lipids after acetone treatment versus untreated controls. Since considerable variation occurred within experimental groups, the values for treated versus untreated side from each group are shown (**Table 1**). In addition, the ratios of the data from the treated versus untreated flanks for each group are shown in Table 1. The untreated control animals showed no difference in mean incorporation into total sphingolipids (μmol/2 h per mg epidermis) between left and right flanks. As expected, the ratio for the untreated control animals (left vs. right sides) was near unity (1.02 ± 0.04). At the first time point after barrier disruption (1–3 h), no significant change in incorporation into sphingolipids was observed between the treated and untreated flanks. Although the synthesis ratio was 1.2 ± 0.2, this difference did not achieve statistical significance. However, by 5–7 h after acetone treatment, a significant increase in [^{3}H]H_2O incorporation into sphingolipids was observed (170%, $P < 0.005$). The incorporation rate remained elevated at the 12–14 h timepoint, and returned toward normal by 22–24 h. These results strongly suggest that disruption of the barrier by acetone produces a burst in total sphingolipid synthesis, which first appears after 5 h and is sustained to at least 24 h.

A comparison of the time course of [^{3}H]H_2O incorporation into sphingolipids (Table 1) with the recovery of epidermal barrier function (**Fig. 1A**) shows that significant barrier repair (35–40%) preceded the acceleration in epidermal sphingolipid synthesis. These results indicate that sphingolipid synthesis increases in response to barrier disruption, but that the response lags behind the early repair of barrier function.

We then determined the relative incorporation of [^{3}H]H_2O into individual sphingolipid species after acetone treatment. Although the incorporation of tritium into total sphingolipids was increased from 5 h onward, the distribution of radioactivity within individual sphingolip-

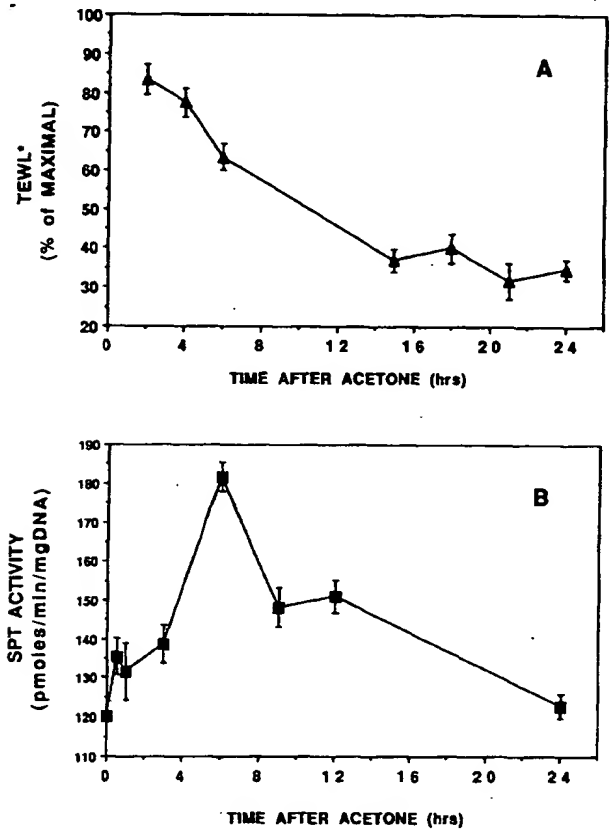

Fig. 1. A: Recovery of epidermal barrier to water loss (TEWL) with time after acetone treatment. Five measurements of TEWL were taken on each of five animals at the indicated timepoints. *Results are presented as the mean percent of the maximal TEWL reading (time 0). B: The total SPT activity versus time. Each point represents the mean SPT activity (± SEM) of triplicate assays determined on at least three separate animals.

id species did not change (**Table 2**). In both treated and normal epidermis, the majority of incorporated tritium appeared in the ceramide and glucosylceramide fractions (≈85%). Sphingomyelin and sphingosine base accounted for far less of the total sphingolipid incorporation (in both treated and untreated epidermis), and this distribution did not change at later time points.

SPT activity after acetone treatment

Since SPT is the rate-limiting enzyme for sphingolipid synthesis (27, 28), we next assessed the alterations in SPT activity induced by disruption of the barrier with acetone (Fig. 1B). The enzymatic activity present in untreated epidermal samples served as the control, which in these experiments was 120 ± 5 pmol/min per mg DNA. Total SPT activity was not significantly increased for the first 5 h after barrier disruption. However, a marked increase occurred at 6 h (≈150%, $P < 0.05$), and enzyme activity remained elevated at 9 and 12 h ($P < 0.05$), with normalization by 24 h after acetone treatment. Moreover, the increase in SPT activity correlated directly with the increased $[^3H]H_2O$ incorporation into sphingolipids at each corresponding timepoint (**Fig. 2**; $r = 0.96$; $P < 0.01$). These studies show that barrier disruption induces an increase in SPT activity after 5 h, which parallels the modulations in $[^3H]H_2O$ incorporation, a measure of in vivo total sphingolipid synthesis. They further suggest that SPT activity accurately reflects total sphingolipid synthesis, and finally that SPT represents a key regulatory step of epidermal sphingolipid synthesis.

Occlusion studies

In order to determine whether the changes in sphingolipid synthesis and SPT activity relate directly to barrier dysfunction, groups of animals first were treated with acetone, and then immediately covered with a water vapor-impermeable Latex^R wrap. As described above, acetone treatment again produced a significant increase in both $[^3H]H_2O$ incorporation into sphingolipids and SPT activity (**Fig. 3**; cf, Table 1 and Fig. 1B). Occlusion of the acetone-treated sites completely inhibited the expected increase in $[^3H]H_2O$ incorporation into sphingolipids 5–7 h after acetone treatment (**Table 3**; Fig. 3A). In contrast, occlusion of normal untreated sites produced no changes in sphingolipid synthesis, suggesting that toxicity from occlusion did not account for the decreased synthesis rates in occluded acetone-treated animals (Fig. 3A). Likewise, the increase in SPT activity that is observed at 6 h after acetone treatment (cf, Fig. 1B) was significantly inhibited

TABLE 2. Distribution of $[^3H]H_2O$ incorporation into sphingolipids

Timepoint	n	Sphingolipid Distribution[a]		
		Sphingomyelin	Sphingosine Base	Glyco + Cer[b]
		lipid weight percent		
Baseline control	16	6.6 ± 0.38	7.2 ± 0.55	85.9 ± 0.75
Acetone-treated (5–7 h)	7	6.5 ± 0.68	6.8 ± 0.23	86.6 ± 0.79
Significance		NS	NS	NS

[a]Defined as the rate of incorporation into individual sphingolipid class/total sphingolipid incorporation × 100; values are mean ± SEM

[b]Represents combined glucosylceramide and ceramide components isolated by HPTLC (see Methods).

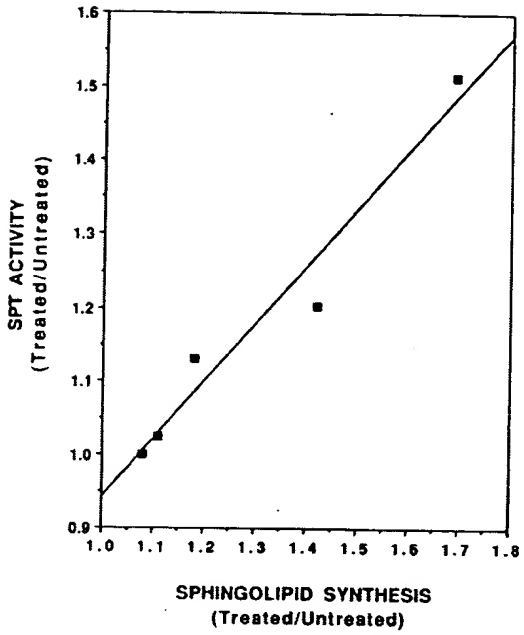

Fig. 2. Correlation between total sphingolipid synthesis and SPT activity after acetone disruption of barrier. The midpoint for each interval of sphingolipid synthesis was compared with the corresponding value for enzyme activity (e.g., 6 h for 5–7 h incorporation interval); $P < 0.01$; $r = 0.96$.

($P < 0.05$) although not completely reversed by occlusion (Fig. 3B). Again, occlusion of normal untreated skin produced no alteration in SPT activity. Finally, occlusion did not change the relative incorporation of $[^3H]H_2O$ into sphingolipid classes (data not shown). These results demonstrate that artificial restoration of barrier function blocks the expected increases in both $[^3H]H_2O$ incorporation into sphingolipids and SPT activity that occur 6 h after barrier disruption.

Other models

To determine whether the observed changes in sphingolipid metabolism are a general phenomenon associated with barrier repair, we next measured SPT activity in two other models of barrier dysfunction. Cellophane tape-stripping of hairless mouse epidermis, which resulted in a rapid and pronounced break in the barrier (TEWL >5.0 mg/cm² per h), also produced an increase in total SPT activity over normal controls (175%, $P < 0.01$ (Fig. 4). Moreover, EFAD animals, which exhibit a chronic abnormality in barrier function showed a nearly 50% increase in SPT activity over normal controls ($P < 0.05$) (Fig. 4). Furthermore, as in the acetone model, occlusion of both tape-stripped and EFAD animals with a vapor-impermeable wrap normalized enzymatic activity in both models (Fig. 4). These studies further confirm that increased sphingolipid production is a general response to barrier requirements in both acute and chronic models of barrier dysfunction.

DISCUSSION

The epidermis contains large quantities of sphingolipids that are concentrated in the stratum granulosum and stratum corneum layers (4–7). Based on a variety of indirect evidence, which is extensively reviewed in the Introduction, it has been hypothesized that the sphingolipids play an important role in the cutaneous permeability barrier. The stratum corneum is also enriched in cholesterol and free fatty acid, and prior studies have shown that cutaneous barrier requirements specifically regulate epidermal cholesterol and fatty acid synthesis (8–10). Recent studies by this laboratory have demonstrated that the activity of SPT is higher in the epi-

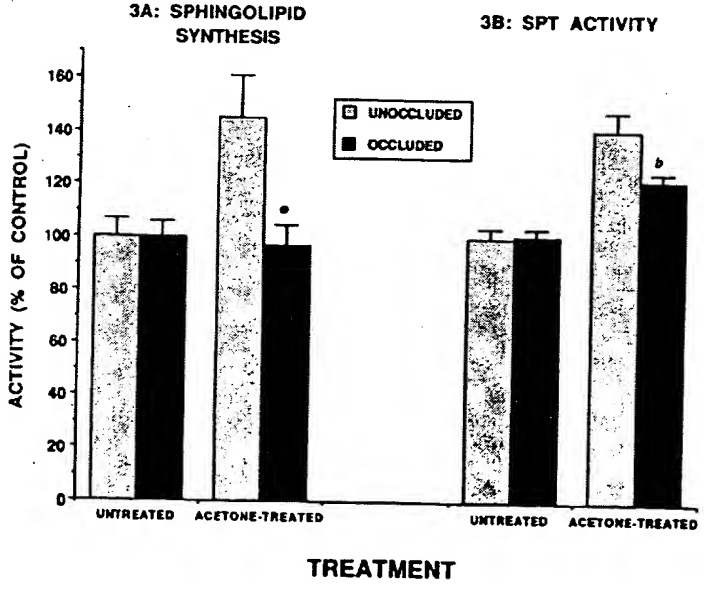

Fig. 3. Effect of occlusion on total sphingolipid synthesis and SPT activity after acetone treatment. In each experiment, two groups of animals were treated with acetone to break the barrier; one group was covered with Latex[R] wrap, while the second group remained uncovered. Activity was plotted as the percent of normal untreated controls for the same experiment; ($n \geq$ four animals in each group; mean ± SEM). A: Sphingolipid synthesis in untreated controls and 5–7 h after acetone treatment. Results from 2 h $[^3H]H_2O$ incorporation are presented for occluded as well as unoccluded animal groups; $^aP < 0.05$. B: SPT activity in untreated normal controls and 6 h after acetone treatment. The occlusive wrap was applied over the entire 6 h in both the untreated and acetone-treated groups; $^bP < 0.05$.

TABLE 3. Effect of occlusion on sphingolipid synthesis 5-7 h after acetone treatment

Description	Synthesis Rate[a]		Significance (P)[b]
	Treated Side	Untreated Side	
	μmol/mg/2 h		
Acetone-treated, unoccluded	4.09 ± 0.44 (n = 4)	2.82 ± 0.20 (n = 4)	<0.05
Acetone-treated, occluded	2.72 ± 0.26 (n = 5)	2.81 ± 0.18 (n = 5)	NS

[a]Mean ± SEM (n).
[b]Determined by paired t-analysis, two-tailed.

dermis than in most other tissues (26), suggesting that sphingolipid synthesis is very active in this site.

In the present study we now demonstrate that sphingolipid synthesis, measured by the incorporation of $[^3H]H_2O$ in vivo, is increased in the epidermis after barrier disruption. This increase in incorporation into sphingolipids returned toward normal with the recovery of barrier function. Moreover, the activity of SPT increased in parallel with the changes in incorporation of tritium into sphingolipids after barrier disruption. We have thus demonstrated a direct correlation between incorporation of tritium into sphingolipids and SPT activity in the epidermis. This provides strong support for the view that SPT is the rate-limiting enzyme in sphingolipid synthesis (26, 27). Of particular note is that the increase in sphingolipid synthesis and SPT activity was seen in two acute models of barrier disruption (acetone and tape-stripping), as well as in one chronic model (EFAD). Additionally, artificial restoration of the barrier with the water-impermeable membrane inhibited the increase in both sphingolipid synthesis and SPT activity. Thus, the observed alterations in sphingolipid metabolism can be considered a specific response by the epidermis to the barrier defect, rather than being attributable to nonspecific toxicity or unrelated effects in each model. Since occlusion normalized SPT activity in all three models, the secondary effects which could occur in each (e.g., acetone: cytotoxicity; tape-stripping: cellular replacement; and EFAD: a general nutritional deficiency) are not likely to be the cause of the observed changes in sphingolipid synthesis.

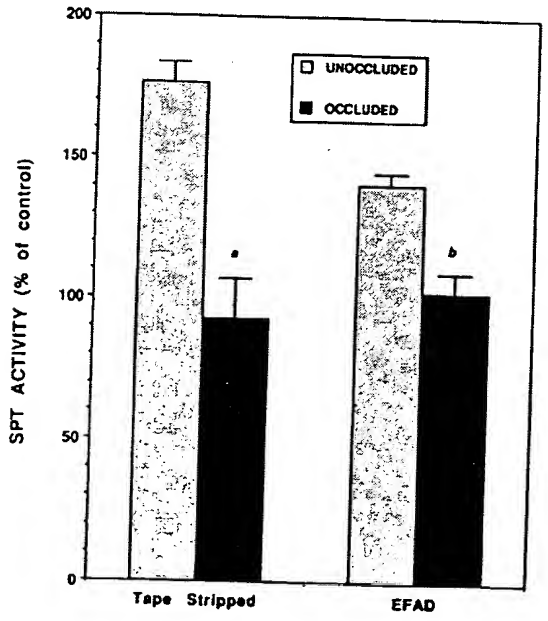

Fig. 4. SPT activity in tape-stripped and EFAD models with and without occlusion. SPT activity is reported as the percent of control SPT levels for each experiment. ($^{a,b}P < 0.01, 0.05$, respectively vs. untreated control). Tape-stripped animals were occluded for 24 h, while EFAD animals were occluded for 72 h.

The results presented here also suggest that de novo sphingolipid synthesis may not be required during the first few hours of barrier recovery, a time period during which up to 60% of barrier recovery has been reported to occur (8, 10, 24, 29). Earlier studies with $[^3H]H_2O$ showed that cholesterol and fatty acid synthesis are both accelerated during the early phases of barrier recovery (0–4 h), returning toward normal levels shortly after 6 h (8, 29). Moreover, the activity of hydroxymethylglutaryl CoA (HMG-CoA) reductase, the rate-limiting enzyme of cholesterol biosynthesis, also increases by 2–3 h after barrier disruption with acetone, returning to normal by 7 h, while the activation state of this enzyme (i.e., dephosphorylated state) increases within the first 30 min after acetone treatment (12). In contrast, the present study demonstrates that neither incorporation of $[^3H]H_2O$ into sphingolipids nor SPT activity increases significantly during the first 5 h after barrier disruption with acetone (Table 1, Fig. 1B). The peak incorporation time for sphingolipids (5–7 h) is quite distinct from that for cholesterol and fatty acids (0–4 h) (8, 29). A lag in precursor pool labeling is not likely to be responsible for this difference in peak incorporation times for a number of reasons. First, the fatty acid pool is the most likely to affect sphingolipid incorporation rates, since ceramides represent the combination of two fatty acid moieties with

a serine molecule. However, the peak in fatty acid synthesis after acetone treatment occurs 3 h prior to peak incorporation into sphingolipids (29). Secondly, the delayed increase in incorporation into sphingolipids correlated well with the activity time course for SPT (Fig. 2). Peak SPT activity (6 h) also corresponded to the peak incorporation time point (5-7 h). From these data we conclude that a delayed increase in sphingolipid synthesis occurs after barrier disruption with acetone. The time course of sphingolipid synthesis after acetone treatment appears quite distinct from cholesterol synthesis in that peak SPT activity and sphingolipid synthesis are observed only after 6 h, while the peak for HMG-CoA reductase activity occurs 3 h earlier.

It has been suggested that the barrier to water loss is more dependent on the structural organization of lipids within the stratum corneum than on the individual lipid species present (34, 35). The data presented here and previously (8–10, 24, 29), as well as recent studies using inhibitors of lipid synthesis, argue that particular lipid species are important for barrier function. Inhibition of epidermal HMG-CoA reductase and cholesterol synthesis with topical lovastatin impaired the immediate recovery of barrier function after acetone treatment (11), confirming that new cholesterol synthesis is required for early barrier repair. Yet, specific inhibition of SPT and sphingolipid synthesis did not influence the same early stages of barrier repair after acetone treatment (36). Together, these studies again suggest a difference in the role of cholesterol synthesis versus sphingolipid synthesis in the early phases of barrier recovery. In addition, these results suggest that a pre-stored pool of sphingolipids in the stratum granulosum may suffice for the early repair of the barrier, and that newly synthesized sphingolipids may not be required for this stage. Rather, the late increase in sphingolipid synthesis may be required either for a later phase of barrier recovery (complete recovery requires 30-36 h) (10), or to provide sphingolipids for replenishment of the storage pool. In contrast, the preformed cholesterol and fatty acid pool in the stratum granulosum cells may not suffice for early repair, and thus synthesis of these two species is stimulated immediately after barrier disruption.

In summary, we have demonstrated for the first time a strong correlation between epidermal sphingolipid synthesis and cutaneous permeability barrier homeostasis. Perturbations of the barrier provoked increased sphingolipid synthesis and SPT activity. However, in contrast to prior descriptions of cholesterol and fatty acid synthesis in the same models, the newly synthesized sphingolipids may not be reqired for the initial phase of barrier recovery, but rather they may be critical to replace depleted storage pools and/or for the replenishment of lipid required for the later stages of barrier recovery.

This work was supported by NIH grants AR-39448, AR-39471, and the Medical Research Service, Veterans Administration. The authors gratefully acknowledge Barbara Brown for her technical assistance, as well as Bil Chapman and Sally Michael for their adroit preparation of this manuscript.

Manuscript received 12 December 1990 and in revised form 4 April 1991.

REFERENCES

1. Elias, P. M. 1983. Epidermal lipids, barrier function, and desquamation. *J. Invest. Dermatol.* **80:** 44–49.
2. Wertz, P. W., and D. T. Downing. 1982. Glycolipids in mammalian epidermis: structure and function in the water barrier. *Science.* **217:** 1261–1262.
3. Yardley, H. J., and R. Summerly. 1981. Lipid composition and metabolism in normal and diseased epidermis. *Pharmacol. Ther.* **13:** 357–383.
4. Gray, G. M., and H. J. Yardley. 1975. Different populations of pig epidermal cells: isolation and lipid composition. *J. Lipid Res.* **16:** 441–447.
5. Gray, G. M., and H. J. Yardley. 1975. Lipid composition of cells isolated from pig, human, and rat epidermis. *J. Lipid Res.* **16:** 434–440.
6. Elias, P. M., B. E. Brown, P. Fritsch, P. Goerke, G. M. Gray, and R. J. White. 1979. Localization and composition of lipids in neonatal mouse stratum granulosum and stratum corneum. *J. Invest. Dermatol.* **73:** 339–348.
7. Lampe, M. A., A. L. Burlingame, J. A. Whitney, M. L. Williams, B. E. Brown, E. Roitman, and P. M. Elias. 1983. Human stratum corneum lipids: characterization and regional variations. *J. Lipid Res.* **24:** 120–130.
8. Menon, G. K., K. R. Feingold, A. H. Moser, B. E. Brown, and P. M. Elias. 1985. De novo sterologenesis in the skin. II. Regulation by cutaneous barrier requirements. *J. Lipid Res.* **26:** 418–427.
9. Feingold, K. R., B. E. Brown, S. R. Lear., A. H. Moser, and P. M. Elias. 1986. The effect of essential fatty acid deficiency on cutaneous sterol synthesis. *J. Invest. Dermatol.* **87:** 588–691.
10. Grubauer, G., K. R. Feingold, and P. M. Elias. 1987. Relationship of epidermal lipogenesis to cutaneous barrier function. *J. Lipid Res.* **28:** 746–752.
11. Feingold, K. R., M. Q. Man, G. K. Menon, S. S. Cho, B. E. Brown, and P. M. Elias. 1990. Cholesterol synthesis is required for cutaneous barrier function in mice. *J. Clin. Invest.* **86:** 1738–1745.
12. Proksch, E., P. M. Elias, and K. R. Feingold. 1990. Regulation of 3-hydroxy-3-methylglutaryl-coenzyme A reductase activity in murine epidermis: modulation of enzyme content and activation state by barrier requirements. *J. Clin. Invest.* **85:** 874–882.
13. Wertz, P. W., D. T. Downing, R. K. Freinkel, and T. N. Traczyk. 1985. Sphingolipids of the stratum corneum and lamellar granules of fetal rat epidermis. *J. Invest. Dermatol.* **83:** 193–195.
14. Elias, P. M., G. K. Menon, S. Grayson B. E. Brown, and S. J. Rehfeld. 1987. Avian sebokeratinocytes and marine mammal lipokeratinocytes: structural, lipid biochemical and functional considerations. *Am. J. Anat.* **180:** 161–177.
15. Prottey, C. 1976. Essential fatty acids and the skin. *Br. J. Dermatol.* **94:** 579–587.
16. Lowe, N. J., and R. B. Stoughton. 1977. Essential fatty acid-deficient hairless mouse: a model for chronic epider-

mal hyperproliferation. *Br. J. Dermatol.* **96:** 155–162.
17. Elias, P. M., and B. E. Brown. 1978. The mammalian cutaneous permeability barrier: defective barrier function in essential fatty acid deficiency correlates with abnormal intercellular lipid deposition. *Lab. Invest.* **39:** 574–583.
18. Bowser, P. A., D. H. Nugteren, R. J. White, U. M. T. Houtsmuller, and C. Prottey. 1985. Identification, isolation and characterization of epidermal lipids containing linoleic acid. *Biochim. Biophys. Acta.* **834:** 419–428.
19. Abraham, W., P. W. Wertz, and D. T. Downing. 1985. Linoleate-rich acylglucosylceramides of pig epidermis: structure determination by proton magnetic resonance. *J. Lipid Res.* **26:** 761–766.
20. Hamanaka, S., C. Asagami, M. Suzuki, F. Inagaki, and A. Suzuki. 1989. Structure determination of glucosyl-β-1-N-(ω-O-linoleoyl)-acylsphingosines of human epidermis. *J. Biochem.* **105:** 684–690.
21. Elias, P. M., B. E. Brown, and V. A. Ziboh. 1980. The permeability barrier in essential fatty acid deficiency: evidence for a direct role of linoleic acid in barrier function. *J. Invest. Dermatol.* **74:** 230–233.
22. Houtsmuller, U. M. T., and A. van der Beck. 1981. Effects of topical applications of fatty acids in essential fatty acid deficiency. *Prog. Lipid Res.* **20:** 219–224.
23. Wertz, P. W., E. S. Cho, and D. T. Downing. 1983. Effects of essential fatty acid deficiency on the epidermal sphingolipids of the rat. *Biochim. Biophys. Acta.* **753:** 350–355.
24. Grubauer, G., K. R. Feingold, R. M. Harris, and P. M. Elias. 1989. Lipid content and lipid type as determinants of the epidermal permeability barrier. *J. Lipid Res.* **30:** 89–96.
25. Imokawa, G., S. Akasaki, M. Hattori, and N. Yoshizuka. 1986. Selective recovery of deranged water-holding properties by stratum corneum lipids. *J. Invest. Dermatol.* **87:** 758–761.
26. Holleran, W. M., M. L. Williams, W. N. Gao, and P. M. Elias. 1990. Serine-palmitoyl transferase activity in cultured keratinocytes. *J. Lipid Res.* **31:** 1655–1661.
27. Braun, P. E., P. Morell, and N. S. Radin. 1970. Synthesis of C18- and C20-dihydrosphingosines, ketodihydrosphingosines, and ceramides by microsomal preparations from mouse brain. *J. Biol. Chem.* **245:** 335–341.
28. Williams, R. D., E. Wang, and A. H. Merrill. 1984. Enzymology of long-chain base synthesis by liver: characterization of serine palmitoyl transferase in rat liver microsomes. *Arch. Biochem. Biophys.* **228:** 282–291.
29. Grubauer, G., P. M. Elias, and K. R. Feingold. 1989. Transepidermal water loss: the signal for recovery of barrier structure and function. *J. Lipid Res.* **30:** 323–333.
30. Bligh, E. G., and W. J. Dyer. 1959. A rapid method of total lipid extraction and purification. *Can. J. Biochem. Physiol.* **37:** 911–917.
31. Feingold, K. R., B. E. Brown, S. R. Lear, A. H. Moser, and P. M. Elias. 1983. Localization of de novo sterologenesis in mammalian skin. *J. Invest. Dermatol.* **81:** 365–369.
32. Bradford, M. M. 1976. A rapid and sensitive method for quantitation of microgram quantities of protein utilizing the principle of protein-dye binding. *Anal. Biochem.* **72:** 248–254.
33. LaBarca, C., and K. Paigen. 1980. A single, rapid, and sensitive DNA assay procedure. *Anal. Biochem.* **102:** 344–352.
34. Friberg, S. E., I. Kayali, W. Beckerman, L. D. Rhein, and A. Simion. 1990. Water permeation of reaggregated stratum corneum with model lipids. *J. Invest. Dermatol.* **94:** 377–380.
35. Potts, R. O., and M. L. Francoeur. 1990. Lipid biophysics of water loss through the skin. *Proc. Natl. Acad. Sci. USA.* **87:** 3871–3873.
36. Holleran, W. M., K. R. Feingold, M. Q. Man., B. E. Brown, and P. M. Elias. 1990. Sphingolipid synthesis in murine epidermis is regulated by permeability barrier requirements. *Clin. Res.* **38:** 635A.

EXHIBIT H

COPY OF (ROUGIER ET AL., *J. INVEST. DERM.*, 81:275-78 (1983)

0022-202X/83/8103-0275$02.00/0
THE JOURNAL OF INVESTIGATIVE DERMATOLOGY, 81:275–278, 1983

Vol. 81, No. 3
Printed in U.S.A.

In Vivo Correlation Between Stratum Corneum Reservoir Function and Percutaneous Absorption

ANDRE ROUGIER, DIDIER DUPUIS, CLAIRE LOTTE, ROLAND ROGUET, AND HANS SCHAEFER

Département de Biologie, Laboratoires de Recherche Fondamentale de l'Oreal (AR, DD, CL, RR), Aulnay sous Bois, and Centre International de Recherches Dermatologiques (HS), Valbonne, France

A relationship between stratum corneum reservoir function and percutaneous absorption has been established in the hairless rat. Two hundred nanomoles of 10 substances that have a wide range of chemical structures were topically applied for 30 min and the total body distribution was measured after 96 h. The quantity of substance present in the stratum corneum reservoir after 30-min application was measured by liquid scintillation counting after tape-stripping the treated area. A linear relationship exists between the quantity of substance in this reservoir x(nmol·cm^{-2}) and the total amount of radioactivity distributed in the body and excreta y(nmol·cm^{-2}) after 96 h. The relationship is given by: $y = 1.644 \times x - 0.536$ ($r = 0.998$, $p < 0.001$). Apart from the steroids, 80–95% of the compounds were excreted in the urine; and with the exception of thiourea, this elimination was rapid, especially for mannitol and benzoic acid.

We confirmed that in terms of penetration there is a factor of 50 between benzoic acid (best) and dexamethasone (worst). Thus the quantity of substance penetrating through intact rat skin can be predicted by measuring the horny layer concentration. The animal data reported here should be verified in humans.

There is considerable evidence to suggest that the most important barrier to drug penetration through the skin is the stratum corneum [1–4], which also acts as a reservoir for molecules applied on the skin [5–7]. These functions then seem closely related [6–9].

The results obtained from various existing methods used for measuring the in vivo penetration, for a given product, are rarely comparable. This is due essentially to the diversity of techniques used, animal species [10,11], anatomical location [1,12], concentration of the molecules tested [13,14], vehicle used [10,15], and duration of the experiment [10]. Furthermore, experience has shown that it is very difficult to extrapolate to humans the results obtained with animals [16–18].

Considering these facts, we asked ourselves, prior to human studies, whether there was a possible relationship between the stratum corneum reservoir function and the molecule penetration in a single species, the hairless rat, under exactly defined experimental conditions.

MATERIALS AND METHODS

Materials

We chose to test molecules having very different physicochemical properties and belonging to different chemical classes. Ten radiolabeled molecules from The Radiochemical Centre Amersham (U.K.) were studied: [1,2-^{3}H]dexamethasone, [1,2,6,7-^{3}H]hydrocortisone, [1,2-^{3}H]-dehydroepiandrosterone, [^{14}C]testosterone, [carboxyl-^{14}C]acetylsalicylic acid, [carboxyl-^{14}C]sodium salicylate, [8-^{3}H]caffeine, [ring-^{14}C]-benzoic acid, D-[1-^{14}C]mannitol, [^{14}C]thiourea.

For each product, a group of 12 female hairless Sprague-Dawley (OFA) rats, aged 12 weeks, weighing 240 ± 10 g was used.

Application Conditions

The molecules were applied on 1 cm^2 of dorsal skin; the animals had previously been anesthetized by 0.5 ml/kg i.p. injection of γ-butyrolactone. The surface of application was delimited by an open circular cell (S = 1 cm^2) fixed by silicone glue (Tecsil). The vehicle, ethanol-water 95/5 (v/v), was chosen according to the solubility of the products with the exception of D-mannitol which was dissolved in ethanol-water 25/75 (v/v) and of sodium salicylate dissolved in ethanol-water 50/50 (v/v).

The standard dose applied was 200 nmol.cm^{-2}, with the exception of benzoic acid which was applied at 200 and 450 nmol.cm^{-2}. The vehicle volatility limits the application period to 30 mins. After this time, the excess product on the applied area was rapidly removed by 2 washings (300 μl) with the vehicle solvent, followed by 2 rinsings (300 μl) with distilled water and light drying with cotton wool.

Conditions for the Percutaneous Absorption Measurements

At the end of the application and washing, the 12 animals were divided into 2 equal groups. The stratum corneum of the application area of the animals from the first group was removed by 6 strippings using "3 M" invisible adhesive tape. Previous histologic studies have shown that this technique removes most of the stratum corneum, the horny layer of the hairless rat skin being composed of 7–8 cellular layers (thickness = 10–15 μm).

The amount of substance contained in the stratum corneum after a 30-min application was determined as follows. The radioactivity on each strip was measured after complete digestion of the keratinic material in Soluene 350 (Packard), addition of Dimilume 30 (Packard), and liquid scintillation counting (Packard 460 C).

The animals of the second group, equipped with collars to prevent licking, were placed individually in metabolism cages for 4 days. During this time, food (Extra Labo) and tap water were provided ad libitum. Urinary excretion was established by daily sampling of the urine and liquid scintillation counting. The feces were collected daily, pooled, and counted by liquid scintillation after lyophilization, homogenization, and combustion of the samples with an Oxidizer 306 (Packard). Four days later, the animals were sacrified by cervical dislocation. Series of 6 strippings were performed on the treated area in order to determine the amount of product not passed through the stratum corneum barrier within 96 h. The remaining skin of the treated area (epidermis + dermis) was sampled and counted by liquid scintillation after digestion in Soluene 350 (Packard). The animals were lyophilized, homogenized, and the samples were counted in liquid scintillation after combustion. For the tritiated molecules, radioactivity in the water of lyophilization was counted, to determine for each case the tritium exchange.

The total amount of substance penetrating in 96 h was determined by adding the amounts found in the excreta (urine + feces), in the epidermis and dermis of the application area and in the whole animal body.

RESULTS

The urinary excretion kinetics of the different substances studied are shown in Table I.

Table II shows the distribution of the tested molecules in urinary and fecal excretions as well as their whole body retention; the penetration rate (illustrated by Fig 1) of the molecules 96 h after their topical application; as well as the amounts of

Manuscript received December 29, 1982; accepted for publication April 11, 1983.

Reprint requests to: Dr. Andre Rougier, Département de Biologie, Laboratoires de Recherche Fondamentale de l'Oreal, 1 avenue de Saint Germain, 93601 Aulnay sous Bois, France.

products present in the stratum corneum at the end of the application period (30 min).

Fig 2 represents the linear relationship between penetration of the substance after 4 days and its level in the stratum corneum at the end of the 30-min application period.

DISCUSSION

The substances tested were chosen because of the wide variety in their structure and physicochemical properties, and because their penetration ability covers a very large range (1–50). The urinary excretion kinetics (Table I) show that, except for thiourea, these substances are rapidly eliminated. This elimination is particularly fast in the case of benzoic acid and D-mannitol. It is important to comment on how the elimination of the substance, particularly by urinary and fecal excretion (Table II). Except for the steroids, the substances tested are eliminated 80–95% by the urinary pathway, although their physicochemical properties differ.

The percutaneous absorption results, in agreement with those obtained in the literature, show that after 96 h there are large differences in the amounts of substances that have penetrated through the skin (Table II, Fig 1). The rank order established in humans by Feldmann et al [19] in the level of steroid penetration—dexamethasone, hydrocortisone, testosterone, and dehydroepiandrosterone—is seen again in our results in rat. Furthermore, hydrocortisone penetrates 5 times less than testosterone and dehydroepiandrosterone which have almost identical penetrating properties. This agreement with the literature is also verified for acetylsalicyclic acid and benzoic acid, the latter known to be very well absorbed [20]. Likewise, it is known that acetylsalicylic acid and salicylic acid have similar penetrating properties [20], whereas their sodium salts exhibit diminished penetration [21] and, indeed, we observed that sodium salicylate penetrates less than acetylsalicylic acid.

It has been established that the penetration of a compound increases with the amount applied [13,14]. This phenomenon has been observed in the case of benzoic acid when applied at 200 and 450 nmol.cm^{-2}.

Despite good agreement of the percutaneous absorption ranking of some substances in animals with the ranking established in humans, extrapolations in absolute values remain problematic. In fact, there are many examples of substances, which, penetrating weakly in animal, can be carried in large amounts through the human skin and vice versa. As an example, in humans, caffeine penetrates approximately 50 times more than thiourea and has almost the same absorption rate as benzoic acid [20]. In the rat, our results have shown that penetrations

TABLE I. *Kinetics of urinary excretion of molecules after topical administration*

Molecules	Urinary excretion (time in hours)			
	0–24	24–48	48–72	72–96
Benzoic acid				
450 nmol·cm^{-2}	61.00[a]	5.60	2.80	1.77
	(2.50)[b]	(0.90)	(0.45)	(0.37)
200 nmol·cm^{-2}	22.95	0.75	0.66	0.43
	(0.55)	(0.06)	(0.07)	(0.04)
Acetylsalicylic acid	3.30	1.20	0.53	0.35
	(0.45)	(0.20)	(0.06)	(0.08)
Dehydroepiandrosterone	0.95	0.43	0.18	0.10
	(0.08)	(0.07)	(0.01)	(0.02)
Sodium salicylate	1.86	0.58	0.60	0.46
	(0.50)	(0.18)	(0.17)	(0.07)
Testosterone	0.92	0.48	0.20	0.14
	(0.29)	(0.07)	(0.04)	(0.02)
Caffeine	1.80	0.39	0.19	0.14
	(0.23)	(0.04)	(0.02)	(0.01)
Thiourea	0.74	0.84	0.30	0.19
	(0.18)	(0.19)	(0.05)	(0.02)
D-Mannitol	1.30	0.09	0.10	0.08
	(0.22)	(0.01)	(0.02)	(0.01)
Hydrocortisone	0.29	0.09	0.06	0.03
	(0.09)	(0.03)	(0.01)	(0.009)
Dexamethasone	0.04	0.035	0.035	0.055
	(0.004)	(0.008)	(0.004)	(0.010)

[a] Expressed in nmol·cm^{-2} application area.
[b] SD (n = 6).

TABLE II. *Parameters of percutaneous absorption of molecules*

Molecules	Total amounts found 96 hours after topical application					Amounts in stratum corneum treated area 30 min after application
	Urine	Feces	Epidermis + dermis area treated	Animal body	Total penetration	
Benzoic acid						
450 nmol·cm^{-2}	71.20[a]	6.25	1.70	0.16	79.30	48.10
	(2.90)[b]	(1.65)	(0.40)	(0.02)	(3.60)	(5.10)
200 nmol·cm^{-2}	24.80	1.32	0.50	0.01	26.60	17.60
	(0.50)	(0.30)	(0.05)	(0.004)	(0.70)	(1.50)
Acetylsalicylic acid	5.40	0.43	0.85	0	6.70	5.15
	(0.70)	(0.15)	(0.20)		(0.70)	(0.64)
Dehydroepiandrosterone	1.67	3.00	0.19	0.43	5.28	1.95
	(0.15)	(0.30)	(0.03)	(0.08)	(0.20)	(0.40)
Sodium salicylate	3.50	0.48	1.00	0	4.98	3.85
	(0.50)	(0.10)	(0.17)		(0.71)	(0.29)
Testosterone	1.72	2.05	0.24	0.33	4.32	2.06
	(0.43)	(0.60)	(0.05)	(0.15)	(0.46)	(0.23)
Caffeine	2.52	0.42	0.15	0.65	3.73	2.76
	(0.25)	(0.07)	(0.01)	(0.06)	(0.30)	(0.34)
Thiourea	2.10	0.76	0.20	0.20	3.23	2.63
	(0.40)	(0.04)	(0.02)	(0.04)	(0.48)	(0.33)
D-Mannitol	1.60	0.42	0.30	0.30	2.63	2.22
	(0.20)	(0.15)	(0.10)	(0.10)	(0.17)	(0.37)
Hydrocortisone	0.46	0.33	0.04	0.03	0.86	0.93
	(0.07)	(0.07)	(0.01)	(0.01)	(0.08)	(0.15)
Dexamethasone	0.16	0.30	0.10	0.04	0.60	0.41
	(0.02)	(0.05)	(0.02)	(0.01)	(0.06)	(0.02)

[a] Expressed in nmol·cm^{-2} application area.
[b] SD (n = 6).

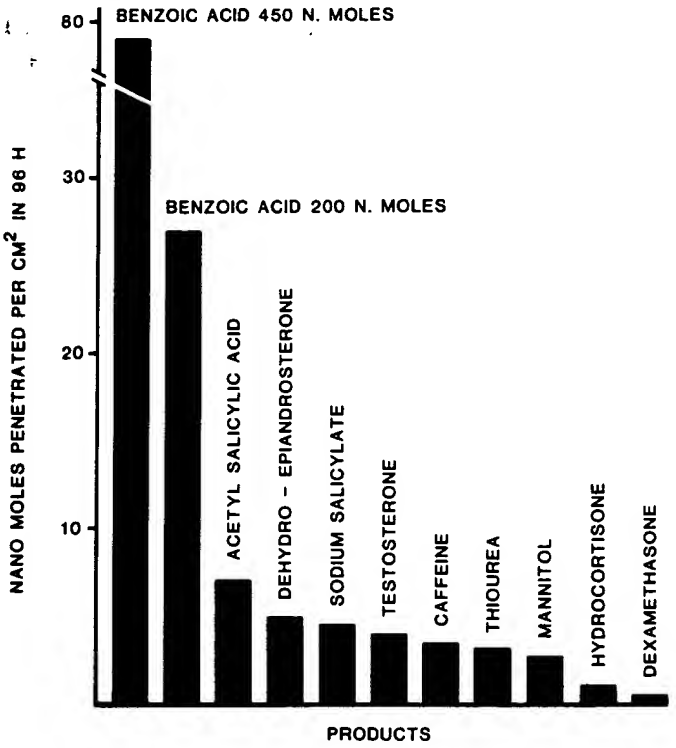

FIG 1. Total percutaneous absorption levels (nmol.cm^{-2}) of the products tested 96 h after their topical application on the hairless rat.

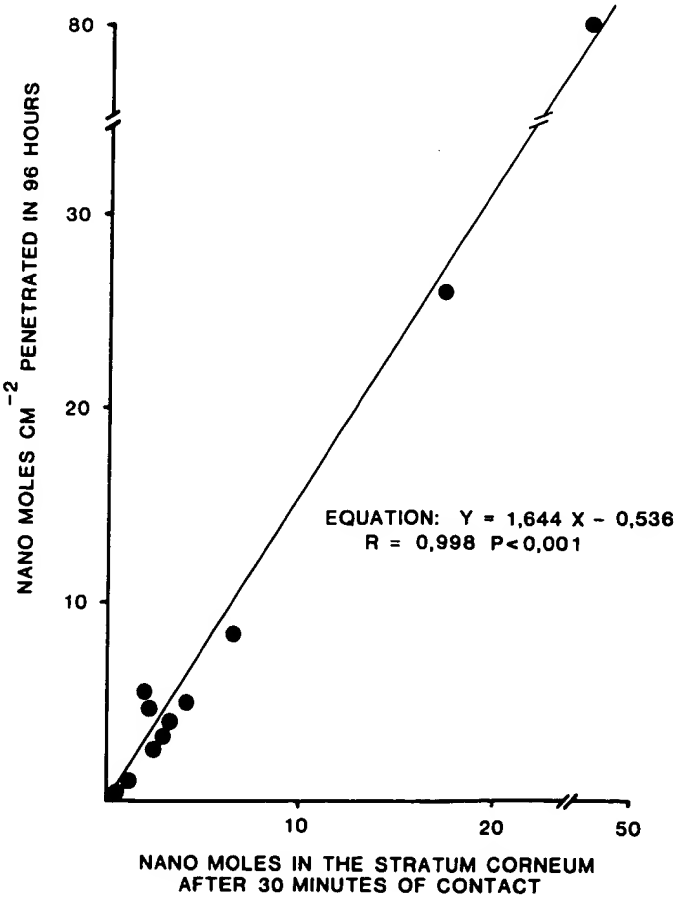

FIG 2. Correlation between the level of penetration of the products after 96 h and their concentration in the stratum corneum after 30 min of application (decimal scale).

of caffeine, testosterone, and thiourea are similar, i.e., 7 times less than that of benzoic acid. These findings clearly illustrate species differences.

The total amount of substances present at the end of application (30 min) in the reservoir constituted by the stratum corneum has been determined by adding the amounts in each strip (Table II). The formation of significant substance reservoir within the horny layer may be due to the existence of differences between the substances in their vehicle-stratum corneum partition coefficients [8,15], to the different permeabilities of the vehicles in which the molecules are solubilized [7,10], to the particular affinity that a compound may have for the horny layer [22,23], or to the combined action of these different factors.

The most important feature of this study is that there is a linear relationship between "the horny layer reservoir effect" at the end of the application period (30 min) (x) and the total amounts of substances penetrating within 96 h (y), independently of the nature of the tested molecule. The linear relationship between the amount of substance penetrating and the amount of substance in the horny layer is of $y = a \times x + b$ type, where $a = 1.644$ and $b = -0.536$ (y and x being expressed in nmol.cm^{-2}). These two variables are correlated with a coefficient of 0.998 and a $p < 0.001$ (Fig 2).

In conclusion, the experimental data show that measuring the amount of a substance within the stratum corneum at the end of the application time (30 min) gives a good prediction assessment of the total amount penetrating in 4 days. This relationship, verified in a single animal species (rat), should now be tested in humans. For technical reasons, the experiments have been carried out using labeled molecules. However, the relatively large amounts of substance present in the "reservoir" of the stratum corneum at the end of the application time should allow penetration studies in both humans and animals, by sensitive nonradioactive techniques.

The authors would like to thank Drs. G. Kalopissis and D. Reymond for their interest and encouragement; M. H. Grandidier, A. M. Cabaillot, and C. Patouillet for excellent technical assistance; J. C. Caron and D. Poisson for the translation and production of the figures.

REFERENCES

1. Marzulli FN: Barriers to skin penetration. J Invest Dermatol 39:387–393, 1962
2. Vinson LJ, Singer EJ, Koehler WR, Lehman MD, Masurat T: The nature of the epidermal barrier and some factors influencing skin permeability. Toxicol Appl Pharmacol 7:7–19, 1965
3. Stoughton RB: Percutaneous absorption. Toxicol Appl Pharmacol 7(suppl 2):1–6, 1965
4. Malkinson FD: Studies on percutaneous absorption of ^{14}C labelled steroids by use of the gas-flow cell. J Invest Dermatol 31:19–28, 1958
5. Malkinson FD, Ferguson EH: Percutaneous absorption. Preliminary and short report. J Invest Dermatol 25:281–283, 1955
6. Vickers CFH: Existence of reservoir in the stratum corneum. Arch Dermatol 88:20–23, 1963
7. Stoughton RB, Fritsch WF: Influence of dimethyl sulfoxide (DMSO) on human percutaneous absorption. Arch Dermatol 90:512–517, 1964
8. Blank IH, Scheuplein RJ: The epidermal barrier, Progress in Biological Sciences in Relation to Dermatology, 2nd ed. Edited by A Rook, RH Champion. Cambridge, Cambridge Univ Press, 1964, pp 245–261
9. Fritsch WF, Stoughton RB: The effect of temperature and humidity on the penetration of ^{14}C acetylsalicylic acid in excised human skin. J Invest Dermatol 41:307–312, 1963
10. Tregear RT: The permeability of skin to molecules of widely differing properties, Progress in Biological Sciences in Relation to Dermatology, 2nd ed. Edited by A Rook, RH Champion. Cambridge, Cambridge Univ Press, 1964, pp 275–281
11. Winkelmann RK: The relationship of the structure of the epidermis to percutaneous absorption. Br. J Dermatol 81(suppl 4):11–22, 1969
12. Lindsey D: Percutaneous penetration, Proceedings of the XII International Congress of Dermatology. Edited by DM Pillsbury, CS Livingood. Amsterdam, Excerpta Medica, 1963, pp 407–415
13. Maibach HI, Feldmann RJ: Effect of applied concentration on

percutaneous absorption in man (abstr). J Invest Dermatol 52:382, 1969
14. Wester RC, Maibach HI: Relationship of topical dose and percutaneous absorption in rhesus monkey and man. J Invest Dermatol 67:518–520, 1976
15. Poulsen BJ: Design of topical drug products: biopharmaceutics, Drug Design, vol IV. Edited by EJ Ariens. New York, Academic Press, 1973, pp 149–190
16. Tregear RT: Physical Function of the Skin. New York/London, Academic Press, 1966
17. Bartek MJ, La Budde JA, Maibach HI: Skin permeability in vivo: rat, rabbit, pig and man. Clin Res 19:358–367, 1971
18. Bartek MJ, La Budde JA, Maiback HI: Skin permeability in vivo: comparison in rat, rabbit, pig and man. J Invest Dermatol 58:114–123, 1972
19. Feldmann RJ, Maibach HI: Percutaneous penetration of steroids in man. J Invest Dermatol 52:89–94, 1969
20. Feldmann RJ, Maibach HI: Absorption of some organic compounds through the skin in man. J Invest Dermatol 54:399–404, 1970
21. Malkinson FD, Rothman S: Percutaneous absorption, Handbuch der Haut und Geschlecht Skrauberten Normale und Pathologische der Haut, vol 1, part 1, Erganzungswerk Bd 1/3. Edited by A Marchionini, HW Spier, Berlin/Gottingen/Heidelberg, Springer, 1963, pp 90–156
22. Blank IH, Gould E: Penetration of anionic surfactants into skin. II. Study of mechanisms which impede the penetration of synthetic anionic surfactants into skin. J Invest Dermatol 37:311–315, 1961
23. Blank IH, Scheuplein RJ: Transport into and within the skin. Br J Dermatol 81(suppl 4):4–10, 1969